Systematic Entomology

Systematic Entomology (2021), DOI: 10.1111/syen.12483

A global phylogenetic analysis of trap-jaw ants, *Anochetus* Mayr and *Odontomachus* Latreille (Hymenoptera: Formicidae: Ponerinae)

ITANNA O. FERNANDES[1], FREDRICK J. LARABEE[2], MARCIO L. OLIVEIRA[1], JACQUES H. C. DELABIE[3] and TED R. SCHULTZ[2]

[1]Instituto Nacional de Pesquisas da Amazônia – INPA, Coordenação em Biodiversidade – COBIO, Manaus, Brazil, [2]Department of Entomology, Smithsonian Institution, National Museum of Natural History, Washington, District of Columbia, U.S.A. and [3]Centro de Pesquisas do Cacau - CEPEC, Laboratório de Mirmecologia UESC/CEPLAC/UFSB, Ilhéus, Brazil

Abstract. We present a phylogeny of the trap-jaw ant genera *Anochetus* and *Odontomachus* with dense taxon sampling representing all biogeographical regions and all species groups for both genera. Four nuclear protein-coding genes (*Long-wavelength rhodopsin*, *Topoisomerase I*, *Wingless* and *Rudimentary*) and one mitochondrial gene (*cytochrome oxidase* I) were sequenced for 221 individuals of *Anochetus* (44 species) and *Odontomachus* (38 species). Analyses using Bayesian and maximum-likelihood criteria recovered essentially the same phylogenetic relationships, including strongly supported reciprocal monophyly of both genera. The analyses recovered nine of the 12 species groups previously proposed for *Odontomachus* and nine of the 22 species groups previously proposed for *Anochetus*. Based on these results, species groups are redefined. *Anochetus* contained an additional new, previously unrecognized group defined here as the hohenbergiae group. Divergence-time analyses estimated the clade composed of *Odontomachus* + *Anochetus* arose during the early Paleocene, with *Odontomachus* and *Anochetus* diverging during the Eocene. Biogeographic analyses suggest that the most recent common ancestor (MRCA) of *Odontomachus* and *Anochetus* occupied either the Neotropical or Afrotropical region during the late Cretaceous and that the two genera radiated during the early Paleocene. The ancestor of *Odontomachus* originated in the Neotropical or Afrotropical regions, giving rise to lineages that radiated during the late Eocene, and the ancestor of *Anochetus* originated in the Neotropical region, giving rise to lineages that radiated during the early Eocene.

Introduction

During the past decade, the higher taxonomic classification of ants (Hymenoptera: Formicidae) has received significant attention (Schmidt, 2013; Schmidt & Shattuck 2014; Brady *et al.*, 2014; Blaimer *et al.*, 2015; Ward *et al.*, 2010, 2015, 2016; Borowiec, 2016). Due to reassessments of morphological variation (Keller, 2011; Schmidt & Shattuck, 2014; Borowiec, 2016) and molecular phylogenetic studies of subfamilies (Schmidt, 2013; Brady *et al.*, 2014; Ward *et al.*, 2015; Borowiec *et al.*, 2019), the higher classification of the subfamilies of Formicidae is now relatively stable. Within those subfamilies, however, uncertainty remains in terms of the relationships within and among major ant genera. This is particularly notable for the large subfamily Ponerinae.

Ponerinae is the third largest subfamily within Formicidae, with 47 genera and more than 1266 valid species and with a worldwide, predominantly pantropical distribution (Schmidt, 2013; Schmidt & Shattuck, 2014; Bolton, 2020). The monophyly of the subfamily was strongly supported in a detailed molecular phylogenetic study by Schmidt (2013),

Correspondence: Itanna O. Fernandes, Instituto Nacional de Pesquisas da Amazônia - INPA. Coordenação em Biodiversidade - COBIO. Av. André Araújo, 2936. Petrópolis, 69067-375. Manaus - AM. Brazil. E-mail: itanna.fernandes@gmail.com

confirming the results of previous molecular phylogenetic studies with more limited sampling of ponerines (*e.g.*, Moreau *et al.*, 2006; Brady *et al.*, 2006). In his molecular phylogeny, Schmidt (2013) recovered *Anochetus* Mayr as a member of tribe Ponerini and sister to *Odontomachus* Latreille, although their reciprocal monophyly could not be proven (see Brown, 1976; Schmidt, 2013). In contrast a subsequent phylogenetic analysis of *Anochetus* and *Odontomachus* by Larabee *et al.* (2016) strongly supported the reciprocal monophyly of both genera.

Anochetus is a large genus with 115 extant and eight fossil species (Bolton, 2020). It is widespread and abundant in the tropical and subtropical regions of the world, with a few species extending into temperate regions. *Anochetus* was erected by Mayr (1861) to contain the ant *Odontomachus ghilianii* Spinola. *Anochetus* has had a stable taxonomic history at the genus level. Although Brown (1973) provisionally synonymized *Anochetus* under *Odontomachus*, he reversed himself (1976) after discovering consistent differences in head structure between the two groups, such as the nuchal carina and apophyseal lines. *Odontomachus* contains 74 extant and three fossil species and, like *Anochetus*, is equally widespread and abundant in the tropics and subtropics. *Odontomachus* also has a stable taxonomic history at the genus level, with three junior synonyms: *Pedetes* Bernstein, *Champsomyrmex* Emery, and *Myrtoteras* Matsumura (Brown, 1976).

The body size of individual *Anochetus* species is generally much smaller than that of *Odontomachus* species, although with some overlap (Larabee & Suarez, 2014). Within and between genera, nesting preferences vary widely, including soil, leaf litter, rotten logs and even the canopy (Raimundo *et al.*, 2009; Cerqueira & Tschinkel, 2010; Camargo & Oliveira, 2012; Feitosa *et al.*, 2012; Shattuck & Slipinka, 2012). Colony size is highly variable across the genus, ranging from an average of only 18 workers in *O. coquereli* Roger (Molet *et al.*, 2007) to as many as 10 000 workers in *O. opaciventris* Forel (De la Mora *et al.*, 2008). Colonies of *Anochetus* are usually smaller, containing fewer than 100 workers (Brown, 1976), though colonies of *A. faurei* Arnold were found to have about 400 workers (Villet *et al.*, 1991). *Anochetus* species also tend to nest and forage more cryptically than the epigaeic *Odontomachus* species; when they do forage above ground, *Anochetus* species are more likely to be nocturnal than are those of *Odontomachus* (Brown, 1978; Schmidt & Shattuck 2014).

Odontomachus and *Anochetus* are remarkable for their trap-like mandibles and associated behaviours, traits that are among the most specialized of any ponerine (Schmidt, 2013; Larabee *et al.*, 2016). In fact, the rapid closure of the trap mandibles is amongst the fastest movement ever measured in any animal (Gronenberg, 1996; Patek *et al.*, 2006; Spagna *et al.*, 2008).

Brown (1978) discussed morphological similarities shared by these two genera, with particular focus on the petiolar node, and he also mentioned that, when considering the intrageneric phylogeny of *Anochetus*, one of the first questions to ask is which species or species group is less derived. Brown (1976, 1978) also created an informal species-groups classification based on morphological similarities that have never been tested. For *Odontomachus*, 12 species-groups (Brown, 1976) and, for *Anochetus*, 22 species groups were created (Brown, 1978), based not only on their morphological similarities but also on their geographic distributions (Table 1).

Despite recent molecular phylogenetic studies on *Anochetus* and *Odontomachus* (Larabee *et al.*, 2016), relationships among the species and species groups created by Brown (1976, 1978) have not been adequately tested. A more detailed phylogenetic analysis, including a large number of species of both genera from all biogeographic regions and representing all of Brown's (1976, 1978) species groups, is necessary for robustly clarifying the relationships within and between the two genera. Using multiple methods, we reconstructed relationships within *Anochetus* and *Odontomachus* to clarify relationships between the genera and among species and to test the monophyly of the informal species groups created by Brown (1976, 1978). We conducted divergence-time and biogeographic analyses to explore the timing and geography of major diversification events on the evolutionary history of this clade of highly specialized ants.

Material and methods

Taxon sampling

Specimens of *Anochetus* and *Odontomachus* were selected to represent a complete phylogenetic sample of the genera, as well as of the species groups, and to encompass as much morphological diversity as possible. Ethanol-preserved or point-mounted specimens were obtained from field collections, collaborators and museum collections. A total of 208 specimens belonging to *Anochetus* (106 specimens, 44 species and 10 species groups) and *Odontomachus* (102 specimens, 38 species and nine species groups), as well as 13 outgroup specimens (11 species spanning the *Odontomachus* genus group *sensu* Schmidt, 2013: *Brachyponera* Emery, *Bothroponera* Mayr, *Leptogenys* Roger, *Megaponera* Mayr, *Mesoponera* Emery and *Odontoponera* Mayr), were included (Table S1). Choice of outgroups was based on previous phylogenetic studies (Schmidt, 2013; Larabee *et al.*, 2016).

Ants were identified primarily using the keys of Brown (1976, 1977, 1978), Sorger (2011), Zettel (2012) and Shattuck and Slipinska (2012), and by comparison to reference collections (Smithsonian Institution National Museum of Natural History and Instituto Nacional de Pesquisas da Amazônia). In several cases, species identity could not be determined from existing keys and samples were either designated with 'cf' for their morphological proximity to described species or given a unique identifier. A full list of taxa, localities, repositories, voucher numbers and GenBank accession numbers are listed in Table S1 (Supporting Information). Specimens from which legs were removed for DNA extraction or from which DNA was nondestructively extracted were deposited at the Smithsonian Institution National Museum of Natural History and Instituto Nacional de Pesquisas da Amazônia or redeposited in the collection from which the specimen was borrowed.

Table 1. Species groups created by Brown (1976) for *Odontomachus* (12 species groups) and by Brown (1978) for *Anochetus* (22 species groups)

Anochetus species group	Species group: Brown (1978)	New species group classification
africanus	***A. africanus*** (Mayr), ***A. bequaerti*** Forel, *A. fuliginosus* Arnold, ***A. madagascarensis*** Forel, *A. natalensis* Arnold, ***A. obscuratus*** Santschi and *A. pellucidus* Emery	***A. africanus***, ***A. bequaerti***, *? ***A. boltoni*** Fisher & Smith, *A. fuliginosus*, *? ***A. goodmani*** Fisher & Smith, ***A. madagascarensis***, *A. natalensis*, ***A. obscuratus*** and *A. pellucidus*.
altisquamis	***A. altisquamis*** Mayr and ***A. orchidicola*** Brown	***A. altisquamis*** and ***A. orchidicola***
bispinosus	***A. bispinosus*** (Smith)	***A. bispinosus*** and *A. chocoensis* Zabala.
cato	***A. cato*** Forel, *A. isolatus* Mann, *A. semininger* Donisthorpe and *A. splendidulus* Yasumatsu	*A. isolatus*, *A. semininger* and *A. splendidulus*
chirichinii	*A. chirichinii* Emery and *A. fricatus* Wilson	*A. chirichinii* and *A. fricatus*
emarginatus	***A. emarginatus*** (Fabricius), *A. haytianus* Wheeler & Mann, ***A. horridus*** Kempf, *A. inca* Wheeler, *A. kempfi* Brown, *A. longispinus* Wheeler, *A. micans* Brown, *A. oriens* Kempf, *A. striatulus* Emery, *A. testaceus* Forel and *A. vexator* Kempf	***A. emarginatus***, *A. elegans* Lattke; *A. haytianus*, ***A. horridus***, *A. inca*, *A. kempfi*, *A. longispinus*, *A. micans*, *A. oriens*, *A. striatulus*, *A. testaceus A. vallensis* Lattke and *A. vexator*
evansi	*A. evansi* Crawley	*A. evansi*
faurei	*A. faurei*	*A. faurei*
gladiator	*A. filicornis* (Wheeler), *A. gladiator* (Mayr) and ***A. variegatus*** Donisthorpe	*A. filicornis*, *A. gladiator* and ***A. variegatus***
graeffei	***A. graeffei*** Mayr, *A. pangens* (Walker) and ***A. yerburyi*** Forel	*A. annetteae* Sharaf, ***A. graeffei***, *A. lanyuensis* Leong *et al.*, *A. pangens*, *? ***A. pattersoni*** Fisher & Smith, *? ***A. pubescens*** Brown, [***A. ruginotus*** Stitz], *A. shohki* Terayama, *A. validus* Bharti & Wachkoo, *? ***A. turneri*** and ***A. yerburyi***.
grandidieri	***A. grandidieri*** Forel, ***A. katonae*** Forel, *A. jonesi* Arnold, *A. punctaticeps* Mayr and ***A. siphneus*** Brown	***A. grandidieri***, ***A. katonae***, *A. jonesi*, *A. punctaticeps*, ***A. siphneus*** and *? ***A. subcoecus*** Forel
ghilianii	*A. angolensis* Brown, ***A. ghilianii*** (Spinola), *A. maynei* Forel, *A. rothschildi* Forel, ***A. rufus*** (Jerdon) and ***A. traegaordhi*** Mayr	*A. angolensis*, ? *A. bytinskii* Kugler & Ionescu, ***A. ghilianii***, *A. maynei*, *A. rothschildi*, ***A. rufus*** and ***A. traegaordhi***
inermis	***A. diegensis*** Forel, ***A. inermis*** André, ***A. simoni*** Emery and ***A. targionii*** Emery	***A. diegensis***, ***A. inermis***, *? *A. miserabilis* González-Campero & Elizalde, ***A. simoni*** and ***A. targionii.***
longifossatus	*A. longifossatus* Mayr, *A. myops* Emery, ***A. pupulatus*** Brown and ***A. subcoecus***	? *A. cryptus* Bharti & Wachkoo, *A. longifossatus*, *A. myops*, ***A. pupulatus*** and *A. schoedli* Zettel
mayri	***A. mayri*** Emery, ***A. minans*** Mann and ***A. neglectus*** Emery	***A. mayri***, ***A. minans*** and ***A. neglectus***
nietneri	*A. consultans* (Walker) and *A. nietneri* (Roger)	*A. consultans*, *? *A. daedalus* Marathe & Priyadarsanan and *A. nietneri*.
pubescens	***A. pubescens***	
rectangularis	*A. armstrongi* McAreavey, ***A. paripungens*** Brown, *A. rectangularis* Mayr and ***A. turneri*** Forel	? ***A. alae*** Shattuck & Slipinska, *A. armstrongi*, ? *A. avius* Shattuck & Slipinska, ***A. paripungens***, *A. rectangularis*, *A. renatae* Mayr, *? *A. rufolatus* Shattuck & Slipinska, *? *A. rufostenus* Shattuck & Slipinska, ? *A. veronicae* Shattuck & Slipinska, *? ***A. victoria*** Shattuck & Slipinska, *? *A. wiesiae* Shattuck & Slipinska
risii	*A. agilis* Emery, *A. brevis* Brown, ***A. incultus*** Brown, *A. modicus* Brown, *A. peracer* Brown, ***A. risii*** Forel, *A. strigatellus* Brown and *A. tua* Brown	*A. agilis*, *A. brevis*, *? ***A. cato***, [*A. gracilis*], ***A. incultus***, *A. leyticus*, ? *A. longus* Chen *et al*, *A. maryatiae* Nuril Aida & Idris, *A. medogensis* Chen *et al.*, *A. modicus*, *A. pangantihoni* Zettel, *A. peracer*, ***A. risii***, *A. strigatellus*, *A. tua* and *A. werneri* Zettel
rugosus	***A. princeps*** Emery, ***A. rugosus*** (Smith) and *A. muzziolli* Menozzi	? *A. mixtus* Radchenko, *A. muzziolli*, *? ***A. princeps***, and ***A. rugosus***.
sedilloti	*A. kanariensis* Forel, *A. levaillanti* Emery, ***A. madaraszi***,Mayr, ***A. obscurior*** Brown, *A. orientalis* André and *A. sedilloti* Emery	*A. kanariensis*, *A. levaillanti*, ***A. madaraszi***, ***A. obscurior***, *A. orientalis* and *A. sedilloti*
talpa	*A. talpa* Forel	*A. talpa*
hohenbergiae		***A. hohenbergiae*** Feitosa & Delabie
***Odontomachus* species groups**	**Species group: Brown (1976)**	**New species group classification**
assiniensis	***O. assiniensis*** Emery	***O. assiniensis***
bradleyi	***O. bradleyi*** Brown	
coquereli	***O. coquereli***	***O. coquereli***
cornutus	*O. cornutus* Stitz	*O. cornutus*
hastatus	***O. hastatus*** (Fabricius)	*? *O. davidsoni* Hoenle *et al.* and ***O. hastatus***.
haematodus	***O. affinis*** Guérin-Méneville, *O. allolabis* Kempf, ***O. bauri*** Emery, *O. biolleyi* Forel, *O. biumbonatus* Brown, ***O. brunneus*** (Patton), ***O. caelatus*** Brown, ***O. chelifer*** (Latreille), ***O. clarus*** Roger, ***O. erythrocephalus*** Emery, ***O. haematodus*** (Linnaeus), *O. insularis* Guérin-Méneville, ***O. laticeps*** Roger, ***O. mayi*** Mann, ***O. meinerti*** Forel, *O. opaciventris*, ***O. panamensis*** Forel, ***O. simillimus*** Smith, *O. spissus* Kempf, ***O. troglodytes*** Santschi and ***O. yucatecus*** Brown	***O. affinis***, *O. allolabis*, ***O. bauri***, *O. biolleyi*, *O. biumbonatus*, ***O. bradleyi***, ***O. brunneus***, ***O. caelatus***, ***O. chelifer***, ***O. clarus***, [*O. desertorum* Wheeler], ***O. erythrocephalus***, ***O. haematodus***, *O. insularis*, ***O. laticeps***, ***O. mayi***, ***O. meinerti***, *O. opaciventris*, ***O. panamensis***, [*O. peruanus* Stitz], ***O. relictus*** Deyrup & Cover, [***O. ruginodis*** Wheeler], ***O. scalptus*** Brown, ***O. simillimus***, *O. spissus*, ***O. troglodytes*** and ***O. yucatecus***

Table 1. Continued

Odontomachus species groups	Species group: Brown (1976)	New species group classification
infandus	***O. angulatus*** Mayr, ***O. animosus*** **Smith**, ***O. banksi*** Forel, *O. florensis* Brown, ***O. infandus*** Smith, *O. latissimus* Viehmeyer, ***O. malignus*** Smith, ***O. papuanus*** Emery, *O. silvestrii* Wheeler *and O. sumbensis* Brown	*O. alius* Sorger & Zettel, ***O. angulatus***, ***O. animosus***, ***O. banksi***, *O. ferminae* General, *O. florensis*, ***O. infandus***, *O. latissimus* *O. litoralis* Wang *et al.*, ***O. malignus***, ***O. papuanus***, [*O. phillipinus* Emery], *O. scifictus* Sorger & Zettel, *O. schoedli* Sorger & Zettel, *O. silvestrii and O. sumbensis*
mormo	*O. mormo* Brown	*O. mormo*
rixosus	*O. latidens* Mayr, ***O. monticola*** Emery and ***O. rixosus*** Smith	*? ***O. circulus*** Wang, [*O. kuroiwae* (Matsumura)], *O. latidens*, ? *O. linearis* Chen & Zhou, *O. minangkabau* Satria *et al.*, ***O. monticola***, *O. pararixosus* Terayama & Ito, [*O. procerus* Emery] and ***O. rixosus***
ruficeps	*O. aciculatus* Smith, ***O. cephalotes*** Smith and *O. ruficeps* Smith	*O. aciculatus*, ***O. cephalotes***, [***O. turneri*** Forel] and *O. ruficeps*
saevissimus	***O. imperator*** Emery, ***O. montanus*** Stitz, ***O. opaculus*** Viehmeyer, *O. rufithorax* Emery and *O. saevissimus* Smith	***O. imperator***, ***O. montanus***, ***O. opaculus***, *O. rufithorax* and *O. saevissimus*
tyrannicus	***O. nigriceps*** Smith, *O. testaceus* Emery and ***O. tyrannicus*** Smith	***O. nigriceps***, *O. testaceus* and ***O. tyrannicus***

Species included in our phylogeny are highlighted in bold. The *Anochetus* species-group hohenbergiae is proposed here for the first time. Question marks '?' indicate that the species was not previously assigned to any species group by prior authors. Asterisk + question mark (*?) indicates a tentative species-group assignment due to uncertainty about whether the species belongs to the indicated species group. The species *O. fulgidus* Wang, *O. granatus* Wang, *O. tensus* Wang and *O. xizangensis* Wang were not included in the list because we did not have access to the descriptions. Brackets [ ] indicate that the status of the species was revised after Brown's studies (1976, 1978) but prior to this one. Species in bold were used in the present study. All species were identified by the first author using Brown's studies (1976, 1978) and the original descriptions or types.

Molecular data

Fragments of four nuclear protein-coding genes were sequenced: *Long-wavelength rhodopsin* (LW Rh), *Topoisomerase I* (TOPI), *Wingless* (Wg) and *Rudimentary* (CAD). A fragment of one mitochondrial gene, *Cytochrome oxidase* I (COI), was also sequenced. Gene fragments CAD, Wg and LW Rh each contain intragenic regions (introns), which were included in the alignment. The primers used to generate the sequence data are listed in Table S2, Supporting Information. It was necessary to divide regions of genes greater than 1 Kb in amplified sequence length into at least two overlapping fragments for amplification and sequencing, including Wg (two fragments), TOPI (two fragments) and CAD (three fragments). These five gene fragments have been successfully used in multiple studies of ant phylogenetics (Brady, 2003; Brady *et al.*, 2006, 2014; Blaimer *et al.*, 2015; Ward *et al.*, 2010, 2015; Blaimer, 2012; Branstetter, 2012; Mehdiabadi *et al.*, 2012; Ward & Sumnicht, 2012; Schmidt, 2013; Cardoso *et al.*, 2014; Larabee *et al.*, 2016; Sosa-Calvo *et al.*, 2017, 2018a, b).

Genomic DNA was extracted destructively or nondestructively using the Qiagen DNeasy Tissue Kit (Qiagen U.S.A., Valencia, CA). In cases of destructive sampling, DNA was extracted from one or two legs taken from a single adult female specimen (usually a worker). Protocols employed for destructive extraction, amplification, and sequencing followed Brady *et al.* (2006), Branstetter (2012), Ward *et al.* (2010), Schmidt (2013) and Blaimer *et al.* (2015). The Qiagen protocol requires cell lysis with 20 μL Proteinase K digestion, which was performed in a 24-h period in this study followed by several steps of DNA binding and purification in mini-column centrifuge tubes. The extracted DNA was eluted from the mini-column in two steps of 50 μL of nuclease-free water each (differing from the Qiagen procedure, which calls for 200 μL of AE buffer). At this point, the eluate (~90 μL) was transferred into clean, sterile, and properly labelled tubes and stored at −20°C. DNA was nondestructively extracted from individuals that were unique, from very limited nest series, and/or otherwise required for future morphological study. Such individuals were either alcohol-preserved or pin-mounted. Nondestructive DNA extractions followed normal extraction procedures, with the exception that the specimens were left intact. During the nondestructive extraction procedure, the entire individual was first dried for 30 min, then placed directly into a 1.5-mL tube with 20 μL of Proteinase K and 180 μL of ATL buffer for 24 h in a thermomixer dry bath at 55°C. After the 24-h cell-lysis process, the complete ant was removed and stored in a vial in 95% ethanol, then cleaned using several washes of ethyl acetate before point-mounting.

DNA sequences were amplified by PCR in 15 μL reaction volumes containing 1 μL of template DNA, 0.4 μL of each 10 μM primer (forward and reverse), 5.7 μL of PCR grade H_2O and 7.5 μL of Promega GoTaq® G2 DNA Polymerase Master Mix (Reaction Buffer [pH 8.5], 1.5 mM $MgCl_2$, 0.2 mM of dNTPs and 1 unit of Taq polymerase; (Promega, Madison, WI, U.S.A.). PCR amplifications were performed in a thermal cycler with the following program: 2–5 min denaturation at 94°C, 35 cycles of 1 min denaturation at 94°C, 1 min annealing at 48–58°C (depending on the primer set) and 1 min extension at 72°C; 1–10 min final extension at 72°C (depending on the primer set) and unlimited hold at 4–10°C.

Visualization of PCR products was performed in ethidium-bromide-stained agarose gel (50 mL of 1.5% TBE gel [Tris/Borate/EDTA] and 1 μL of ethidium bromide) by running 3 μL of product mixed with 1.5 μL of 6X loading dye and were run for ~30 min at 100 volts. PCR product was then purified by adding 1.6 μL of the enzymatic cleanup reagent ExoSAP-IT® (Affymetrix Inc., Santa Clara, CA, U.S.A.; exonuclease I and shrimp alkaline phosphatase), previously diluted in nuclease-free water (9:1), into the remaining 10–15 μL of

PCR product; then the solution was run in a thermal cycler for 30 min at 37°C, for enzyme to remove unincorporated nucleotides and primers, followed by 15 min at 80°C, for enzyme inactivation. Sequencing reactions used 1 μL of the cleaned PCR product. Bi-directional sequencing reactions were performed at the Laboratories for Analytical Biology (LAB) of the Smithsonian Institution National Museum of Natural History on an ABI 3100 automated sequencer using BigDye Terminator v3.1 Cycle Sequencing kit (Applied Biosystems Inc., Foster City, CA, U.S.A.). Sequence data were assembled and edited using the program Geneious v. 8.1.6 (Biomatters Ltd., Auckland, New Zealand).

Alignment and sequence annotation

All DNA sequence fragments were assembled in Geneious v7.1 (Biomatters Ltd.) using the DeNovo tool, and their identities were confirmed by BLAST search against the National Center for Biotechnology Information - NCBI nucleotide database. The 5′-to-3′ orientation of fragments was determined automatically by the program, but in cases where the program was in error, sequences were reversed and/or complemented. Not all sequences were complete. The CAD sequences of several species, in particular, contained numerous long introns, necessitating the use of three overlapping amplicons employing the following primer combinations: (1) CD847F/CD1465R nested with CD847F/CD1459R; (2) CD1276F/CD1879R nested with CD1421F/CD1879R; and (3) CD1679F/CD2362R nested with CD1821F/CD2362R. In these cases, CAD sequences were only partially obtained due to recalcitrant amplification in some taxa (Larabee *et al.*, 2016).

Gene fragments were aligned using the program MAFFT v.7 (Katoh, *et al.*, 2009) as implemented in Geneious v7.1. Nucleotide sequences were translated into amino acid sequences in Mesquite v.3.3 (Maddison & Maddison, 2015) and compared to amino acid sequences in the NCBI database both as an additional confirmation of gene identity and to ensure correct codon reading frame. Noncoding regions (i.e., introns) were aligned using the online version of the program MAFFT v.7 (Katoh *et al.*, 2002; Katoh *et al.*, 2009; Katoh & Toh, 2010; Katoh & Standley, 2013) maintained by the Computational Biology Research Center of the National Institute of Advanced Industrial Science and Technology (AIST, Japan: http://mafft.cbrc.jp/alignment/server/). Noncoding intron regions were not included for the outgroup taxa in order to maximize the number of informative sites for the ingroup taxa.

For coding regions, alignments were performed using the AUTO strategy, which, depending on the dataset, selects the most appropriate strategy, and the scoring matrix for nucleotide sequences was set to 1PAM/K = 2, which is suggested for closely related DNA sequences. For other parameters (*gap opening penalty* and *offset value*), the default settings were used (1.53 and 0.0, respectively). Alignment of noncoding regions (introns) was performed under the iterative refinement method (FFT-NS-i) in which an alignment is obtained first by conducting progressive alignment, then is subjected to an iterative refinement process (Berger & Munson, 1991; Gotoh, 1993; Katoh *et al.*, 2002; Katoh *et al.*, 2009; Katoh & Toh, 2010; Katoh & Standley, 2013). The MAFFT alignment was then submitted to the guide-tree based alignment GUIDANCE web-server (Penn *et al.*, 2010); http://guidance.tau.ac.il/) with the GUIDANCE2 algorithm chosen for assessing confidence values of the alignment (Sela *et al.*, 2015; Privman *et al.*, 2012). The GUIDANCE2 algorithm uses a bootstrapped guide tree (100 pseudoreplicates), generates an alignment for each tree and then assigns a confidence score for each site in the alignment of the observed data based on its consistency across the bootstrap-based alignments. This confidence score was used to determine which positions in the variable noncoding regions to exclude (mask) from further analyses (Sosa-Calvo *et al.*, 2018b). We used an arbitrary, somewhat rigorous, 90% bootstrap value as a cutoff to identify sites that were poorly aligned. Sites that were considered poorly aligned (in addition to those sites previously identified by the guidance algorithm) were also excluded from further analyses. Gene fragments were concatenated in Geneious v7.1 (Biomatters Ltd.) and inspected by eye in Mesquite v.3.3. The concatenated aligned data matrix for these genes was 4258 bp in length.

Phylogenetic inference

Our original dataset consisted of 245 specimens, but many of those were missing more than one gene fragment and the distribution of bootstrap support values strongly suggested that a subset of the specimens with missing values were behaving as ‘rogue’ taxa (Aberer *et al.*, 2011). In order to identify and account for the effects of such taxa, we employed the online version of the program RogueNaRok (http://rnr.h-its.org), which takes as input the ML best tree and the set of ML bootstrap trees. The best results came from their single-taxon algorithm, which begins by removing taxa one at a time to find the taxa (if any) whose deletion most improves the scores.

Based on RogueNaRok results for the full 245-taxon dataset, (specimens) we experimented with analyses from which various combinations of rogue taxa (specimens) were excluded, ultimately settling on the dataset of 221 specimens that is the primary focus of this paper (Table S1, Supporting Information). This focal dataset excludes 24 specimens in which missing data were significantly negatively affecting phylogenetic analyses (Table S3, Supporting Information).

The program PartitionFinder was again employed to identify best-fitting data partitions and substitution models (comparing all 56 models of evolution; ‘models = all’) in order to avoid over-parameterization, which has been shown to cause strong bias in posterior probability (PP) estimation (Lanfear *et al.*, 2012; Lemmon & Moriarty, 2004). Input partitions (‘data blocks’) included each of the three codon positions for each of the four nuclear protein-coding genes (12 partitions); one intron each for Wg and LW Rh and three introns for CAD (five partitions); and each of the three codon positions of the mitochondrial gene (three partitions), for a total of 20 data blocks. Two analyses were conducted in PartitionFinder using

the Bayesian information criterion, the '*greedy*' algorithm and a user tree obtained from a RAxML 8.1.3 (Stamatakis, 2014) analysis of the unpartitioned data. The analyses differed in that one evaluated all 56 available models of nucleotide evolution, whereas the other evaluated only those available in RAxML (results summarized in Table S4, Supporting Information).

Using the resulting partitions and models (or, in cases where a model was unavailable, the next-most-complex model available), Bayesian analyses were carried out using the MPI (parallelized) version of the program MrBayes v.3.2.2 (Ronquist *et al.*, 2012, 2013) with the following settings: *nucmodel = 4by4*, *nruns = 2*, *nchains = 8*, *samplefreq = 1000* and *20 million generations*. In order to avoid known problems with branch-length estimation (Marshall, 2010; Marshall *et al.*, 2006), branch-length priors were set as follows: *prset applyto = (all) brlenspr = unconstrained:exponential* (*100*). All parameters except topology and tree length were unlinked across data subsets by using the command *prset applyto = (all) ratepr = variable*. Burn-in and stationarity were assessed by comparing the potential scale reduction factor values and split-frequency diagnostic in MrBayes and by examining effective sample size (>200) values and the mean and variance of log likelihoods, both by eye and by using the Bayes Factor comparison in Tracer v1.6 (Rambaut & Drummond, 2007). Based on this information, burn-in was set at two million generations. Clade support was assessed by combining the post-burn-in trees and generating a 50% majority-rule consensus tree with PPs in FigTree 1.4.2 (Rambaut, 2014).

Using the PartitionFinder results for RAxML models and all models, respectively, maximum-likelihood best-tree and bootstrap analyses were carried out in the programs RAxML v7.7.7 (Stamatakis, 2014) and GARLI v.2.0 (Zwickl, 2006, 2011). Depending on the partition, RAxML analyses utilized GTR + G and GTR + G + I models (Table S4) and a combined best-tree and bootstrap analysis with 1000 rapid bootstrap pseudoreplicates. Garli ML best-tree analyses consisted of 1000 pseudoreplicates and deviated from default settings as follows: *genthreshfortopoterm = 5000; scorethreshforterm = 0.10; startoptprec = 0.5; minoptprec = 0.01; brlenweight = 0.002; numberofprecreductions = 1; topoweight = 0.01; treerejectionthreshold = 20.0*. In GARLI analyses the value for *modweight* was calculated as 0.0055 × (#subsets + 1) (Zwickl, pers. comm.). Bayesian analyses were carried out using parallel processing (one chain per CPU) on the Smithsonian NMNH AntLab AtomAnt 12-core Intel-processor Apple computer; RAxML analyses were carried out on the Smithsonian NMNH AntLab AntPAC computer cluster and GARLI analyses were carried out on the Smithsonian OCIO Hydra supercomputer.

Divergence dating

We inferred divergence dates for the five-gene dataset with the program BEAST 2.3.2 (Bouckaert *et al.*, 2014). Unlike more common node-calibration models that use influential *ad hoc* probability distributions for node age priors, the fossilized birth–death (FBD) process incorporates speciation rate (λ), extinction rate (μ), fossil recovery rate (ψ) and the proportion of sampled extant species (ρ) as parameters in a single comprehensive model for estimating node ages (Stadler, 2010; Heath *et al.*, 2014). This provides a way to integrate fossil dates into the tree estimation process and potentially provides more accurate dating estimates than node-calibration methods (Larabee *et al.*, 2016).

Table 2. Partitions and models identified by PartitionFinder adapted to the models used by BEAUTi for the 221 specimens +12 fossils (233 specimens) of the 4258 bp concatenated dataset

Subset	Gene fragment block	BEAUTi Models	Frequency (base)
p1	TOPIpos1, TOPIpos2, Wgpos1, Wgpos2	TN93	Estimated
p2	CADpos3, TOPIpos3	TN93	All equal
p3	CADpos1, Wgpos3	TN93	All equal
p4	LWpos3	HKY	Estimated
p5	COIpos1, LWpos1	GTR	Estimated
p6	COIpos2, LWpos2	TN93	Estimated
p7	CADpos2	TN93	Estimated
p8	COIpos3	HKY	All equal
p9	CADintron1, CADintron2, CADintron3, LWintron, Wgintron	HKY	Estimated

All introns were directed to the same partition (p9).

The XML files used in the analysis were created using BEAUTi and edited manually through the text editor. The FBD analyses used as priors the results of previous dating analyses for the genera *Odontomachus* and *Anochetus* (Schmidt, 2013; Larabee *et al.*, 2016). The partitioning scheme and the models used in BEAUTi are summarized in Table 2. Two independent Markov chain Monte Carlo (MCMC) analyses were performed, each with a length of 200 million generations, with parameters sampled every 10 000 generations. The FBD analysis was conducted with a *diversification rate* of 0.06, *turnover* and *sampling proportion* of 0.5 and *Rho* of 0.6, based on the number of *Anochetus* and *Odontomachus* species used in the analysis. The *prior* for the diversification rate (*diversificationRate*) was 0.06 with an exponential prior distribution with *mean* 1.0. The origin was configured with a *relaxed log-normal clock* starting with 75 Ma (*Odontomachus* genus group) with *mean* (M) 50 and *standard deviation* set to (S) 0.25 and *offset* of 20.0. Because the program requires that well-defined clades be fixed *a priori* for the analyses, we used clade topologies resulting from the MrBayes analyses.

The precise calibration of molecular clocks to estimate divergence times depends critically on the interpretation of paleontological information (fossils), particularly in the dating of the fossils and in their phylogenetic placement (Arcila *et al.*, 2015). Fossils are typically used in molecular phylogenetics as sources of information about prior minimum or maximum ages of internal nodes (Asher *et al.*, 2002, 2003; Donoghue, 1989; Kumar & Hedges, 1998; Zuckerkandl, 1987). Twelve fossil species were used to calibrate nodes in the BEAST analysis, including eight species of *Anochetus*, three species of *Odontomachus*, and one

Table 3. Fossil species, their respective species groups, and references used for divergence-dating calibrations using FBD model

Fossil species	Taxon or Clade	Age (Ma)	Reference
Anochetus ambiguus De Andrade	species groups emarginatus	17	Dominican Amber (De Andrade, 1994)
Anochetus brevidentatus Mackay	species groups inermis	17	Dominican Amber (Mackay, 1991)
Anochetus conisquamis De Andrade	species groups cato	17	Dominican Amber (De Andrade, 1994)
Anochetus corayi Baroni Urbani	species groups mayri	17	Dominican Amber (Baroni Urbani, 1980)
Anochetus dubius De Andrade	species groups emarginatus	17	Dominican Amber (De Andrade, 1994)
Anochetus exstinctus De Andrade	species groups emarginatus	17	Dominican Amber (De Andrade, 1994)
Anochetus intermedius De Andrade	species groups inermis	17	Dominican Amber (De Andrade, 1994)
Anochetus lucidus De Andrade	species groups altisquamis	17	Dominican Amber (De Andrade, 1994)
Odontomachus paleomyagra Wappler *et al.*	Clade A	20	Czech Impression Fossil (Wappler *et al.*, 2014)
Odontomachus pseudobauri De Andrade	species groups haematodus	17	Dominican Amber (De Andrade, 1994)
Odontomachus spinifer De Andrade	species groups haematodus	17	Dominican Amber (De Andrade, 1994)
Leptogenys lacerata Zhang	*Leptogenys*	17	Chinese Impression Fossil (Zhang, 1989)

species of *Leptogenys* (Table 3), but the prior distributions for fossil ages were not defined because these ages are estimated as part of the FBD model during the analysis. The convergence of each run was evaluated by examining effective sample size values (>200), PPs and consistency of likelihood values resulting from several independent runs in Tracer 1.6. The first 100 million generations were discarded as burn-in, and the maximum clade credibility tree was summarized in TreeAnnotator 2.2.1 (Drummond *et al.*, 2012). The resulting topology and divergence times were visualized using FigTree v1.4.0. BEAST analyses were carried out using the CIPRES Science Gateway (Miller *et al.*, 2010).

Biogeographic analyses

The ancestral geographic distributions of *Odontomachus* and *Anochetus* were estimated using the BioGeoBEARS R package (BioGeography with Bayesian and Likelihood Evolutionary Analysis in R Scripts) (Matzke, 2013), which tests different approaches based on biogeographic models. BioGeoBEARS allows probabilistic inference of both historical biogeography (ancestral geographic ranges on a phylogeny) as well as comparisons of different models of range evolution.

The BioGeoBEARS package features a variety of models that describe vicariance, speciation events and founder-event speciation. Two input files were submitted to BioGeoBEARS, one of them in .txt (geogfn) containing information related to the specimens (e.g., name of the species and biogeographic region in which it occurs) and the tree obtained from the BEAST (FBD) analysis in Newick format, saved from Mesquite. For the analyses, we implemented the standard two-parameter dispersal and extinction cladogenesis (DEC) model (Ree & Smith, 2008), as well as the DEC + J version of the model that incorporates founder-event speciation by assigning a separate probability parameter 'j' (Matzke, 2014), following the guidelines and tutorials available on the BioGeoBEARS PhyloWiki (http://phylo.wikidot.com/biogeobears). The starting value for the founder-event speciation parameter 'j' was specified with jstart = 0.0001.

Each *Anochetus* and *Odontomachus* species was assigned to one or more of the six biogeographic regions previously defined by Cox (2001): Neotropical (T), Nearctic (N), Afrotropical (F), Indomalayan (I) (comprises Indian subcontinent and Southeast Asia west of Wallace's Line), Paleartic (P) and the Australasian region (A) (comprises Australia, New Guinea, New Zealand and Pacific islands east of Wallace's Line). Region assignments were based on information from antmaps.org (Guénard *et al.*, 2017), widely used by myrmecologists, as well as specimen locality labels. In total, we analyzed 233 specimens (including fossils) distributed in six biogeographic regions of the world, with the maximum areas observed for the same taxon equal to three.

BioGeoBEARS also allows the addition of an extra parameter in the models that predicts the occurrence of dispersal followed by speciation via founder event (model + J) and also a dispersion multiplier, which can be switched off (M0), allowing equal transitions between any areas over time, or switched on (M1), allowing higher transition rates for dispersions in one direction, which is generally used for island biogeography and therefore was not used in the present study. This implementation is relevant due to the fact that speciation via founder event has been shown to be a crucial process in several clades investigated, although it is better measured in island systems (Matzke, 2014).

Results

Anochetus and Odontomachus phylogeny

All analyses and partitioning schemes, including Bayesian (Figs 1 and 2), maximum likelihood with both RAxML (Supplemental Fig. S2) and GARLI (Supplemental Fig. S2), resulted in trees with similar relationships for *Anochetus* and *Odontomachus* species (see discussion). Bayesian posterior probabilities (BPPs) and bootstrap (BS) support values are summarized in Table 4. To simplify discussion of support values from the various analyses, we use the following acronyms: Bayesian posterior probabilities (BPP), maximum-likelihood RAxML (rBS) and maximum-likelihood GARLI (gBS). Our analyses recovered nine species groups previously defined by Brown for *Odontomachus* and nine previously defined by him for *Anochetus*

(Brown, 1976, 1978) (Table 1). Based on these results, we have divided the two genera into 10 clades (*Odontomachus* A–E/*Anochetus* F–J; Figs 1 and 2).

The same outgroup topology, including the relationships of some species of the *Odontomachus* genus group, was recovered in both likelihood (RAxML and GARLI) analyses, but the results of the Bayesian analysis differed in the positions of *Brachyponera* and *Bothroponera*. All three analyses agreed on the topology of the *Odontomachus* genus group (*sensu* Schmidt, 2013) containing the genera *Leptogenys*, *Megaponera*, *Mesoponera* and *Odontoponera*. All analyses recovered *Odontoponera transversa* as the sister group of *Odontomachus* + *Anochetus*, with low support for the maximum-likelihood bootstrap values (gBS: 49, rBS: 60) and high support for the BPP (0.98). The *Odontomachus* + *Anochetus* clade had high support values in all analyses (gBS: 97, rBS: 100 and BPP: 1), supporting the monophyly of the clade containing the two genera.

In the genus *Odontomachus*, clade A (Fig. 1), consisting of Afrotropical species in the assiniensis species group, is strongly supported (gBS: 99, rBS: 100, BPP: 1). Clade B includes Afrotropical, Paleartic and Indomalayan species belonging to the coquereli + rixosus species groups and is supported by low bootstrap support values (gBS: 6, rBS: 75) but by a high PP (BPP: 97). Clade C contains Neotropical species belonging to the hastatus species group and, as in Larabee *et al.* (2016), was recovered with consistently high support values (gBS: 100, rBS: 100, BPP: 1). Clade D, composed of Indomalayan and Australasian species belonging to the tyrannicus + ruficeps and saevissimus + infandus species groups, is also well supported (gBS: 100, rBS: 100, BPP: 1). The last *Odontomachus* clade (E) consists of Neotropical, Nearctic and Afrotropical species, all belonging to the haematodus species group, and is moderately well supported by maximum-likelihood (gBS: 84, rBS: 85) and very well supported by Bayesian (BPP: 0.99) analyses (Fig. 1).

Within *Anochetus*, clade F, containing Neotropical species belonging to the hohenbergiae species group (newly defined for this study), is the sister group of the previously defined altisquamis species group and is maximally well supported (gBS: 100, rBS: 100 and BPP: 1). The species *A. hohenbergiae* was described in Feitosa *et al.* (2012) and is here included in a phylogenetic analysis for the first time. Clade G is composed of the risii and rugosus (*A. rugosus* + *A. risii*) species group, consisting of Indomalayan species, and is supported by strong support values (gBS: 100, rBS: 100, BPP: 1). Clade H, consisting of Neotropical species belonging to the emarginatus species group, is supported by low bootstrap values (gBS: 69, rBS: 78), but by a high posterior probabilities (BPP: 98). Like clade H, clade I also consists exclusively of Neotropical species in the bispinosus, inermis and mayri species groups and is strongly supported (gBS: 94, rBS: 98, BPP: 1). The largest clade in the genus *Anochetus*, clade J, is composed of Afrotropical, Paleartic, Australasian and Indomalayan species belonging to the sedilloti, grandidieri, graeffei, rectangularis, africanus, ghilianii, longifossatus, rugosus and gladiator species groups and is generally well supported (gBS: 86, rBS: 96, BPP: 1).

Our analyses support nine of the species groups for the genus *Odontomachus* and nine for *Anochetus* created by Brown (1976, 1978), and a tenth in *Anochetus*, the hohenbergiae species group, created here (Table 1).

Divergence dating

The root (stem) node subtending (*Odontomachus* + *Anochetus*) was estimated as 81.5 Ma (HPD: 62.2–106.4 Ma), with an origin in the Cretaceous. The crown node subtending *Odontomachus* + *Anochetus* was estimated as 64.8 Ma (HPD 49.8–82.3 Ma) in the early Paleocene. The estimated crown-group origin of *Odontomachus* is 51.4 Ma (HPD 37.4–66.9 Ma) in the early Eocene, and the estimated crown-group origin of *Anochetus* is 53.9 Ma (HPD 42.6–68.1 Ma), also during the Eocene. The results of clade-origin analyses are summarized in Table 5, and the chronogram is presented in Fig. 3.

Clades A and B belonging to the group of species assiniensis, coquereli and rixosus diverged approximately 34.2 Ma (HPD 23.2–47.4 Ma) during the Oligocene. Clades C and D, belonging to the hastatus, tyrannicus, ruficeps, saevissimus and infandus species groups, respectively, diverged approximately 28.7 Ma (HPD 21.5–37.8 Ma) during the late Oligocene. The last clade (E) for the genus *Odontomachus*, belonging to the haematodus species group, had diverged approximately 19.7 Ma (HPD 17.0–24.5 Ma) during the early Miocene. *Odontomachus* diversified 30–19 Ma, during the Oligocene and early Miocene.

Clade F, composed of the hohenbergiae and altisquamis species groups, was originated 35.7 Ma (HPD 22.2–50.7 Ma) during the early Oligocene. Clade G diverged from clade F 53 Ma and is composed of the risii and rugosus species groups, which originated 25.7 Ma (HPD 17.0–41.6 Ma) during the late Oligocene. Clade H, containing the emarginatus species group, originated 30.1 Ma (HPD 22.2–39.4 Ma) during the Oligocene. Clade I, containing the bispinosus, inermis and mayri species groups, originated 29.5 Ma (HPD 22.6–37.7 Ma) during the Oligocene. Clade J, consisting of the sedilloti, grandidieri, graeffei, rectangularis, africanus, ghilianii, longifossatus, rugosus and gladiator species groups, originated 44.4 Ma (HPD 34.6–57.0 Ma) in the Eocene. *Anochetus* diversified between 44 and 25 Ma, beginning in the Eocene, as indicated in the FBD model tree (Fig. 3).

Biogeographic reconstruction

Both models (DEC and DEC + J) suggested that the MRCA of *Odontomachus* and *Anochetus* arose in the Neotropical or Afrotropical region during the late Cretaceous, radiating during the early Paleocene (~65 Ma). Support values for DEC + J (LnL = −321.5; AICc = 649.2; d: 0.0031; e: 7.60E−10; j: 0.0066) compared to those for DEC (LnL = −327.9; AICc = 659.8; d: 0.0038; e: 0.0006; j: 0) indicated that the former does not provide a significantly better fit to the data, with the exception of the founder event as expected. We therefore

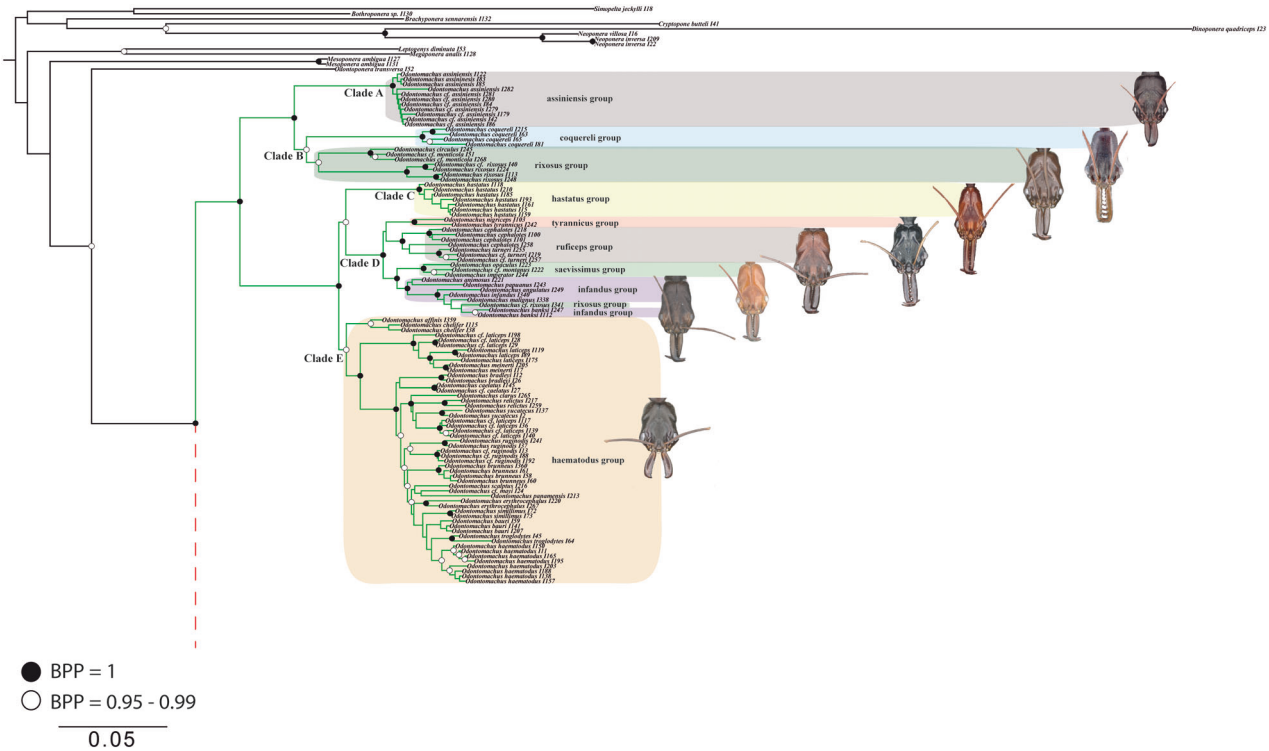

Fig. 1. Phylogeny of trap-jaw ants in the genus *Odontomachus* (green branches) based on Bayesian analysis conducted in MrBayes. Outgroups are represented by black branches. The phylogeny of the sister genus, *Anochetus* (dashed red line), is continued in Fig. 2. Nodal support values indicate Bayesian posterior probabilities (BPPs). Clades as described in the text are indicated by letters (A–E). Species groups discussed in the text are indicated by coloured boxes. Ant images were obtained and edited from AntWeb, Version 8.41, California Academy of Science, online at https://www.antweb.org. Accessed 2 July 2020. [Colour figure can be viewed at wileyonlinelibrary.com].

focussed our discussion on the results estimated from the standard DEC + J model.

Analyses indicated that *Odontomachus* arose in the Neotropical or Afrotropical regions, dispersing in the late Eocene (~37 Ma). Species in the genus *Anochetus* share an MRCA that originated in the Neotropical region and radiated during the early Paleocene (~58 Ma), earlier than the estimated radiation of *Odontomachus*. Clades A and B, consisting of species from the Afrotropical, Indomalayan and Palearctic regions, radiated during the late Eocene (~ 37 Ma) and share an MRCA that originated in the Afrotropical region. Clades C, D and E share an MRCA that lived in both the Neotropical and Autralasian regions during the Eocene (~37–58 Ma), subsequently giving rise to lineages that dispersed to the Autralasian, Indomalayan, Afrotropical and Nearctic regions also during the late Eocene (~37 Ma) (Fig. S3).

Clades F and G, containing Neotropical and Indomalayan species, shared an MRCA in the Neotropical region, which gave rise to a lineage that dispersed to the Indomalayan region during the Paleocene (~58 Ma). Clades H, I and J shared an MRCA that occupied the Neotropical and Indomalayan regions during the late Paleocene (~58 Ma), giving rise to daughter lineages that dispersed to the Palearctic, Afrotropical and Australasian regions during the Eocene (58–37 Ma) (Fig. S3).

Discussion

Phylogeny compared with the species groups of Brown (1976, 1978), divergence and biogeography

The topologies produced in all analyses (Bayesian, RAxML and GARLI) are very similar with regard to the ingroup, varying only in the positions of hohenberigae species group in the RAxML analyses, which recovered the risii + rugosus species group as the sister group of all *Anochetus* species, with low support (rBS: 26). Some outgroup species in Bayesian analyses (*Bothroponera*, *Brachyponera* and *Cryptopone*) were also varying. The monophyly of *Odontomachus* and *Anochetus* are each very well supported (*Odontomachus*: BPP: 1, gBS: 98, rBS: 100; *Anochetus*: BPP: 1, gBS: 98, rBS: 100), contradicting some previous studies (Moreau & Bell, 2013; Schmidt, 2013), but agreeing with Larabee *et al.* (2016). All of our analyses recovered *Odontoponera* as the sister group of (*Odontomachus* + *Anochetus*), with low support from maximum-likelihood (gBS: 49, rBS: 60) but high support from Bayesian analyses (BPP: 0.98). The maximum-likelihood analyses of Larabee *et al.* very weakly recovered (BS: 21) *Pseudoneoponera* as the sister group of *Anochetus* + *Odontomachus*, whereas their Bayesian analyses recovered *Phrynoponera* as the sister group, again

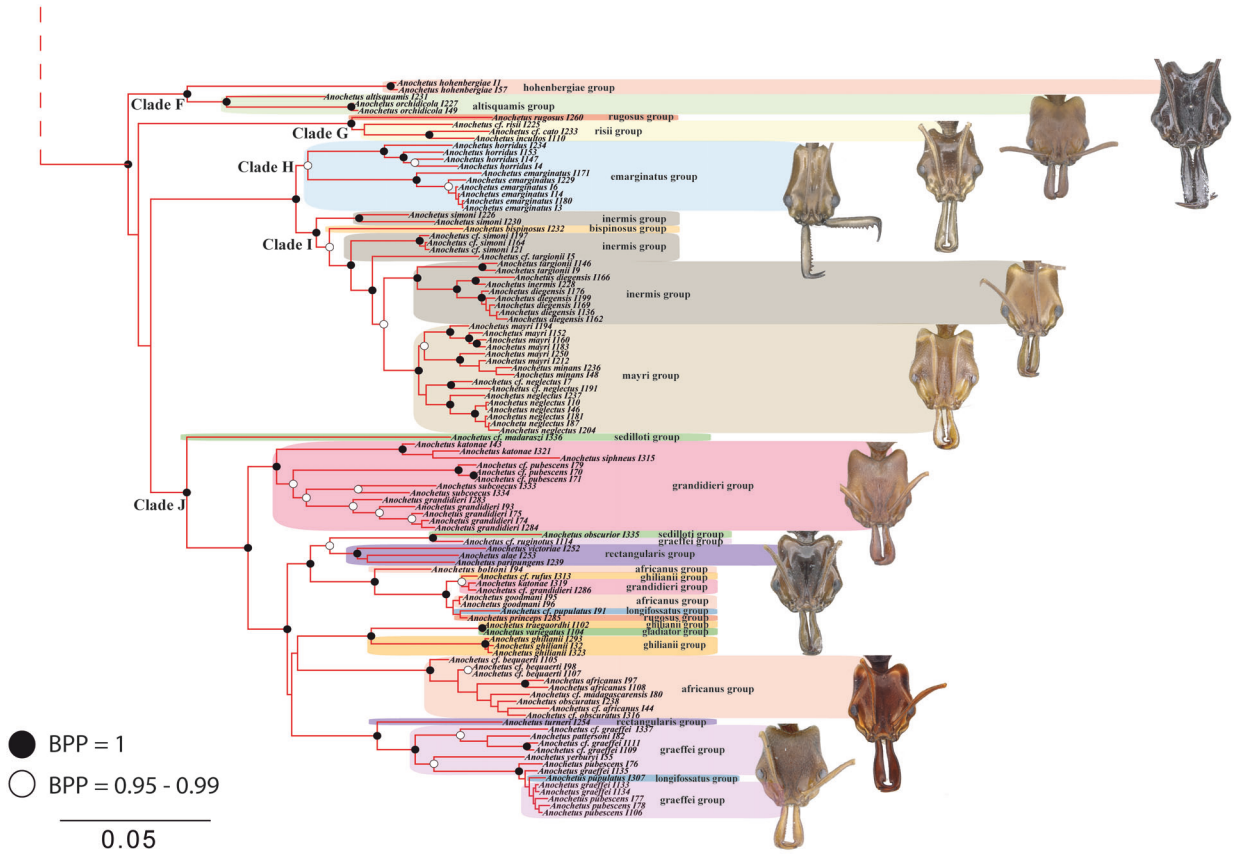

Fig. 2. (continued from Fig. 1). Phylogeny of trap-jaw ants in the genus *Anochetus* (red branches) based on Bayesian analysis conducted in MrBayes, continued from Fig. 1. Nodal support values indicate BPPs. Clades as described in the text are indicated by letters (F–J). Species groups discussed in the text are indicated by coloured boxes. Ant images were obtained and edited from AntWeb, Version 8.41, California Academy of Science, online at https://www.antweb.org. Accessed 2 July 2020. [Colour figure can be viewed at wileyonlinelibrary.com].

with low support (BPP: 58), as did a Bayes factor comparison of the results of two constraint analyses. In their divergence-dating analyses, Larabee *et al.* (2016) recovered *Mesoponera* and *Odontoponera* as the sister group of *Anochetus* + *Odontomachus*. Recently, in a study of the effects of compositional heterogeneity, Borowiec *et al.* (2019) presented a phylogeny of Formicidae using 11 genes. They found that compositional heterogeneity indeed appears to affect the placement of the root of the ant tree, suggesting that outgroup choice should not only be based on close relationship to the ingroup but should also take into account sequence divergence and other properties relative to the ingroup. Larabee *et al.* (2016) recovered only five *Odontomachus* species groups and six *Anochetus* species groups for a total of 93 specimens (ingroup). Our work has a total of 208 specimens belonging to *Anochetus* (106 specimens) and *Odontomachus* (102 specimens), more than double the number used by Larabee *et al.* (2016), which highlights the importance of including as many specimens as possible in order to accurately reconstruct ingroup relationships. Adequately testing the sister-group question will require the inclusion of more representatives of the *Odontomachus* genus group.

Larabee *et al.* (2016) estimated that the MRCA for *Odontomachus* + *Anochetus* originated around 52.5 Ma (39.4–62.7 HPD) during the Eocene, whereas estimates from the present study indicate an origin in the late Paleocene. We found that the MRCA of *Odontomachus* + *Anochetus* diverged around 64.8 Ma (HPD 49.8–82.3 Ma) in the early Paleocene. The crown-group origin of the genus *Odontomachus* was estimated as Eocene (51.4 Ma) (Fig. 3), whereas Larabee *et al.* (2016) estimated it to be about 40 Ma. The crown-group origin of *Anochetus* was estimated at 53.9 Ma (HPD 42.6–68.1 Ma), earlier than that estimated for *Odontomachus*, but also during the Eocene and earlier than the estimate of Larabee *et al.* (2016), 45 Ma. Diversification rate was estimated to be 0.06 in the present study, close to the estimate found for the *Odontomachus* + *Anochetus* in a study of diversification rates for Ponerinae (Moreau & Bell, 2013). Most infrageneric clades (A–J) are considered young (5.5–44 Ma) and are subtended by short branch lengths, suggesting that some groups have undergone rapid radiations in the last 30 Ma (Fig. 3).

The DEC + J analyses indicate that the common ancestor of *Anochetus* + *Odontomachus* originated in the Afrotropical or Neotropical region and subsequently radiated

Table 4. Support values from Bayesian (BPP) and maximum-likelihood (RAxML [rBS] and GARLI [gBS]) analyses for selected clades of the genera *Anochetus* and *Odontomachus*

Clade	MrBayes (BPP)	RAxML (rBS)	Garli (gBS)
Odontomachus + *Anochetus* + *Odontoponera*	0.98	60	49
Odontomachus + *Anochetus*	1	100	97
Odontomachus	1	100	98
Anochetus	1	100	98
Clade A	1	100	99
Clade B	0.97	75	64
Clade C	1	100	100
Clade D	1	100	100
Clade E	0.99	85	84
Clade F	1	100	100
Clade G	1	100	100
Clade H	0.98	78	69
Clade I	1	98	94
Clade J	1	99	91

Table 5. Crown-group age estimates for major clades of the genus *Odontomachus* and *Anochetus*

Clade	FBD (HPD = higher posterior density)	BEAST: BPP = Bayesian posterior probability
Odontomachus + *Anochetus* + *Odontoponera*	81.5 (62.2–106.4)	0.63
Odontomachus + *Anochetus*	64.8 (49.8–82.3)	1
Odontomachus	51.4 (37.4–66.9)	1
Anochetus	53.9 (42.6–68.1)	1
Clade A	3.99 (0.5–4.)	1
Clade B	30.2 (20.8–41.5)	0.61
Clade C	5.5 (2.9–9.4)	1
Clade D	19.4 (17.0–24.5)	1
Clade E	19.7 (17.0–24.5)	1
Clade F	35.7 (22.2–50.7)	1
Clade G	25.7 (17.0–41.6)	0.98
Clade H	30.1 (22.2–39.4)	1
Clade I	29.5 (22.6–37.7)	1
Clade J	44.4 (34.6–57.0)	1

FBD = fossilized, birth–death. HPD = highest posterior density (95%) and BPP = Bayesian posterior probability. Ages in millions of years (Ma).

to other regions. Larabee *et al.* (2016) estimated that *Anochetus* + *Odontomachus* originated in the Neotropical or Indomalayan region, also based on the DEC model. A study of *Leptomyrmex* spider ants similarly supports a Neotropical origin with dispersal to Australia (Boudinot *et al.*, 2016). A route through Antarctica could explain the radiation of *Anochetus* and *Odontomachus* ancestors originating in the Neotropical region during the late Cretaceous. The divergence of these lineages probably occurred in the Paleocene (65–58 Ma), when Africa had already completely separated from the block formed by Australia, Antarctica and South America.

Odontomachus

In his study of *Odontomachus*, Brown (1976) mentioned that the genus apparently arose from a primitive *Anochetus* species, based on morphological characters of the posterior vertex and the apophyseal line, present on the head of *Odontomachus* but absent in *Anochetus*. Data from karyotypes (Santos *et al.*, 2010) and adductor muscle morphology (Gronenberg & Ehmer, 1996) support this scenario, with *Anochetus* possessing ancestral states of both characters (posterior vertex and the apophyseal line). Other aspects of morphology have apparently evolved more rapidly in *Anochetus* than in *Odontomachus*, including body size, reduction in eye size and reduced pigmentation associated with cryptobiosis in *A. myops*, *A. talpa* and *A. minans*. *Odontomachus* species have a larger average body size and tend to occupy exposed ground-surface and arboreal adaptive zones (Brown, 1976). Basally diverging species such as *A. emarginatus* and *A. hohenbergiae* retain the plesiomorphic character states of larger body size, large eyes and mandible with a series of large teeth and are clearly adapted to arboreal life.

Odontomachus clades A and B include species belonging to the assiniensis, coquereli and rixosus species groups, considered morphologically typical for the genus, with teeth finely serrated along the mandibular border, well developed temporal prominences and conical petioles. Our results corroborate those of Larabee *et al.* (2016) with regard to species groups as well as to uncertainty about the identification of some species such as *O. assiniensis*, indicated in our phylogeny by 'cf. assiniensis'. Our morphological study of *O. assiniensis* found large variation in the pattern of striae on the mesosoma and in the form of the petiole, suggesting the possibility of cryptic species occurring in sympatry in localities in Uganda (Fig. 1).

The assiniensis species group contains only the single described species and exhibit broad heads, reduced jaws and smooth and shiny gasters; these characters are shared with species of the rixosus group, represented in our analyses by the species *O. rixosus* and *O. monticola*. A close relationship between these groups was suggested by Brown (1976) and is

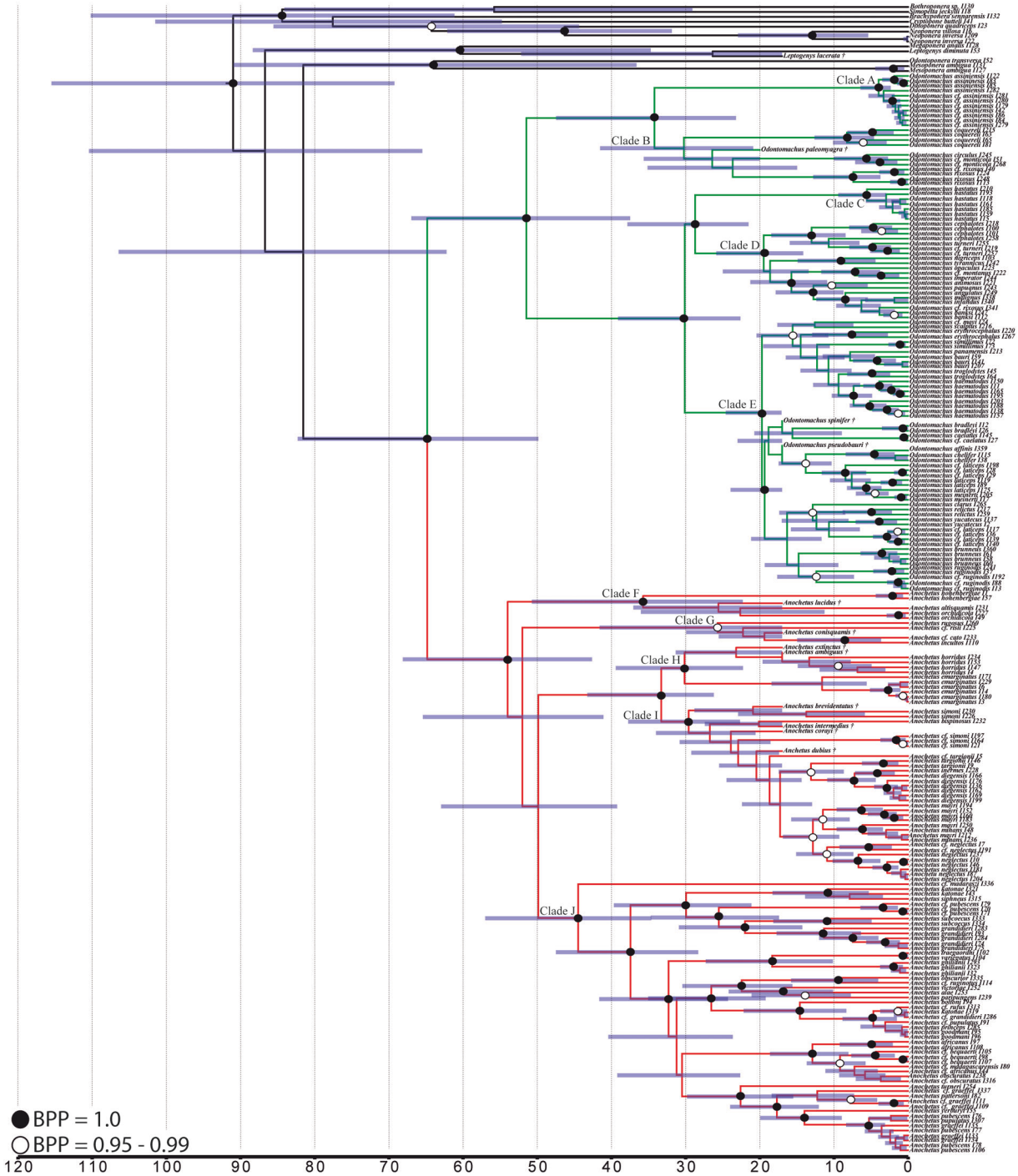

Fig. 3. Maximum credibility tree resulting from an FBD (fossilized, birth–death) analysis for the genera *Anochetus* (red branches) and *Odontomachus* (green branches) conducted in BEAST. Mean node ages are illustrated with highest posterior density (95%) (HPD) (blue bars). Node support is indicated by BPP (Bayesian posterior probability). Ages are in millions of years ago (Ma). [Colour figure can be viewed at wileyonlinelibrary.com].

supported by our phylogeny. Based on morphology, we have included *O. circulus* in the rixosus species group.

The coquereli species group, also containing a single species, is particularly distinct with respect to the well-developed subapical teeth, conical head with no temporal prominences and the slender and long petiole. Previous studies had suggested that *O. coquereli* is the sister of *Anochetus* (Schmidt, 2009), thus rendering *Odontomachus* paraphyletic. Brown (1976) considered

O. coquereli to be closely related to the tyrannicus species group, but our results, as well as those of Larabee *et al.* (2016), contradict that hypothesis.

In our analysis, the fossil species *O. paleomyagra* was used to calibrate the ancestor of the A + B clade (Fig. 3) based on morphological characteristics shared with members of that clade, with an estimated minimum age of 20 Ma, the age of the Czech amber. Based on this and other calibrations, the origin and diversification of clades A and B were estimated at 34 and 30 Ma, respectively, similar to that found by Larabee *et al.* (2016). The ancestor of clades A and B occupied the Afrotropical region, with descendant lineages subsequently dispersing into the Afrotropical, Palearctic and Indomalayan regions.

Recently, Hoenle *et al.* (2020) described a new species, *O. davidsoni*, from Ecuador. In their molecular analyses, the morphologically similar *O. hastatus* (clade C) was found to be the sister of the new species. Both share relatively large size, red to brown colouration, head in dorsal view with a large difference between ocular and vertexal widths, relatively slender habitus and a bilobed metasternal process. Based on morphological and molecular evidence, we assign *O. davidsoni* to the hastatus species group. Clade C is sister to clade D, comprising the tyrannicus, ruficeps, saevissimus and infandus species groups. All of the species groups in clades C and D (Fig. 1) were previously proposed by Brown (1976). *O. hastatus* is morphologically similar to the species of the saevissimus species group, as noted by Brown (1976), who also emphasized the close relationship between the Old and New World species. Here we include *O. turneri* in the ruficeps species group, a placement that is also supported by the results of Larabee *et al.* (2016). The infandus, saevissimus and tyrannicus species groups are morphologically similar, sharing the presence of long, acute, apical intercalar and subapical mandibular teeth and a series of smaller preapical teeth. The analyses also recovered one species of *O.* cf. *rixosus* within the infandus species group, thus rendering the infandus group paraphyletic. Brown (1976) proposed likely ancestral traits shared by the saevissimus, tyrannicus and coquereli species groups, including the shape of the head, long jaws with long and sharp apical teeth and an elongated and pointed petiole, something also observed in the hastatus species group. If these character states are indeed ancestral; then, the more derived character states of the mouthparts and head present in all three groups may be homoplasious.

No fossil data were available to calibrate clades C and D because there are no known fossils that share the morphological characteristics of the extant species. Our analyses indicate that the stem-group ancestor of those clades originated around 28 Ma, with a crown-group age of around 19 Ma. The ancestor of clade C was Neotropical, dispersing in the late Oligocene (24 Ma) (Fig. S3). The ancestor of clade D arose in the Neotropical region during the Eocene, giving rise to lineages that subsequently dispersed to the Indomalayan and Australasian regions during the late Oligocene (24 Ma).

Matos-Maraví *et al.* (2018), suggest that non-neutral processes have played an important role in generating the extant diversity and distribution of Indo-Pacific (Indomalayan and Australasian) *Odontomachus* species. In a test of Wilson's (1959, 1961) taxon-cycle hypothesis, they found that the Melanesian *Odontomachus* (tyrannicus, ruficeps, saevissimus, and infandus species groups) arose from a New World lineage rather than from Southeast Asian rainforest ancestors, as previously proposed by Wilson (1959, 1961). The initial dispersal event into Melanesia, according to Matos-Maraví *et al.* (2018), took place in the early Miocene, most likely as a direct long-distance dispersal event across the Pacific Ocean. They hypothesized that sporadic trans-Pacific dispersal has possibly contributed to the present-day assemblage of *Odontomachus* Melanesian fauna.

Larabee *et al.* (2016) also concluded dispersal to the Afrotropical and Indomalayan regions from the Neotropical region, where *O. hastatus* occurs. Our analyses, in agreement with Larabee *et al.* (2016), suggest that the ancestor probably occupied the Neotropical region and gave rise to lineages that subsequently radiated to the Old World at the beginning of the Eocene while retaining the shared morphology observed in the tyrannicus, ruficeps, saevissimus, and infandus species groups. As suggested by Moreau & Bell (2013) and Pie (2016), the New World was essential for generating and maintaining the biodiversity of ants, partly because of the high plant diversity in this region.

Clade E, the largest species group in the genus, contains the haematodus species group. We included in our analyses the largest number of species possible in order to test the monophyly of the group as proposed by Brown (1976), including two Old World species *O. simillimus* and *O. troglodytes* (Fig. 1). The species in the haematodus group share the presence of well-developed temporal prominences, relatively short jaws with blunt apical teeth and a conical petiolar node. Brown (1976) mentioned the possibility of subgroups of species within the haematodus group, including a subgroup containing *O. mayi*, *O. affinis* and *O. panamensis*, which share a smooth vertex. Our analyses support a subgroup containing *O. chelifer* and *O. affinis*, which are morphologically distinct from other species in the haematodus species group. *O. chelifer* has a strongly elongated head and curved-transverse striae on the dorsum of the gaster, whereas all other members of the haematodus group have short heads and lack transverse striations on the gaster. Support values for clade E, which includes *O. chelifer*, are relatively strong (BPP: 1, rBS: 85, gBS: 84), but to clarify relationships between the species in the group, more species need to be included in future analyses. The inclusion of *O. allolabis* could shed light on the relationships of *O. affinis* and *O. chelifer*.

Clade E was calibrated with the fossils *O. spinifer* and *O. pseudobauri* (Fig. 3), both from Dominican amber, which is estimated to be 17 Ma old. The origin of clade E was estimated at 19 Ma, rapidly diversifying at 18 Ma, as also observed by Larabee *et al.* (2016). Based on the DEC analysis, at least one subsequent dispersal into the Afrotropical and Indomalayan regions from the Neotropical region occurred in clade E, which mostly contains Neotropical species belonging to the haematodus species group but also contains *O. troglodytes* and *O. simillimus* (Afrotropical and Indomalayan/Australasian, respectively) and the Nearctic species *O. relictus*.

Anochetus

The clades within *Anochetus* have high support values in key areas but lack support in others (Fig. 2). Clade F includes species in the hohenbergiae and altisquamis species groups and is sister to the rest of the genus. Ants in the altisquamis species group, containing *A. altisquamis* and *A. orchidicola*, are relatively small and robust, with a high, rounded petiolar node apex that is sometimes emarginate. The hohenbergiae species group contains the single species *A. hohenbergiae* Feitosa & Delabie, previously placed in the emarginatus species group. We place this species in a species group separate from the altisquamis species group based on its distinctive morphological characteristics such as abundant pilosity, posterior margin of the head strongly concave, mandibles with a row of 13–16 teeth, unarmed propodeum and a conical and spiniform petiole. This last character is similar to that of *Odontomachus* species, making *A. hohenbergiae* distinctive amongst other *Anochetus* species. Additional characters supporting the placement of *A. hohenbergiae* near the base of *Anochetus* include the configuration of the head, particularly of the posterior vertex and apophyseal lines, forming shelf-like internal muscle attachments that are well developed in *Odontomachus* but not in *Anochetus* (Brown, 1976) and also by the form of the petiole.

The gladiator species group, which contains relatively large-sized species, was suggested as a possible link between *Anochetus* and *Odontomachus* by Brown (1978) and Larabee *et al.* (2016). Brown (1976) hypothesized that the ancestor of *Anochetus* was probably a large, epigeic ant. Larabee *et al.* (2016) did not include representatives of the gladiator species group in their analyses but hypothesized that large-sized *Anochetus* species have evolved several times independently. Our results indicate that, rather than an early-diverging lineage, the gladiator species group, represented here by *A. variegatus*, is highly derived within *Anochetus*. *Anochetus variegatus* and the closely related *A. ghilianii* comprise a species group that is the sister clade of the africanus species group (Fig. 2).

Clade F, which is represented by the fossil *A. lucidus* from Dominican amber (dated to 17 Ma), was estimated to have originated 35 Ma, almost coincident with the origin of crown-group *Odontomachus* (34 Ma). Clade F is a good example of the retention of plesiomorphic morphological characters that are shared with some *Odontomachus* species in the Afrotropical and Neotropical regions, except for the absence of the apophysial line (diagnostic character), indicating the possible parallel evolution of some subsequently evolved characters, because the two genera diversified simultaneously (51–53 Ma).

Clade G is composed of the rugosus and risii species groups and is strongly supported (BPP: 1, rBS: 100, gBS: 100). Brown (1978) suggested a close relationship between these two species groups based on the relatively conical and pointed petiolar node. In addition to the conical petiole, both the *A. risii* and *A. rugosus* groups have long jaws (dentate in *A. rugosus*) and bodies with abundant pilosity (characteristics also observed in the hohenbergiae species group), as well as rugose sculpture. Larabee *et al.* (2016) indicated that *A. princeps* and *A. rugosus* belong to the rugosus group, but the two species are morphologically very different in sculpture and petiole shape. The rugosus species group was found in our analyses to be polyphyletic, with *A. princeps* closely related to some African species. The resolution of the rugosus species group (which includes *A. muzzioli*) will require the inclusion of more species.

Clade G, which was calibrated with the species *A. conisquamis* from Dominican amber (dated to 17 Ma), originated around 25.7 Ma, a result similar to that of Larabee *et al.* (2016), who estimated an origin of 24.1 Ma. Clade G, containing the rugosus and risii species groups, was reconstructed with an Indomalayan origin. According to Boudinot *et al.* (2016), overland dispersal with subsequent Antarctic extinctions is roughly corroborated by similar minimum age estimates of ∼30 Ma for trans-Antarctic interchanges of multiple arthropod groups, including chironomid midges (Krosch *et al.*, 2011), colletid bees (Almeida *et al.*, 2012), euophryine spiders (Zhang & Maddison, 2013), window flies (Winterton & Ware, 2015) and various stoneflies (McCulloch *et al.*, 2016).

Clade H is formed by species belonging to the emarginatus species group and is supported by low bootstrap values (gBS: 69, rBS: 78), but by a high posterior probabilities (BPP: 0.98). Species in this group are large and elongate (Total Length: ∼10–12 mm), the mandibles possess a series of teeth (3–16) and the petiole can be short or long (*A. longispinus*) and is bidentate, with two spines separated from one another. The emarginatus species group was poorly represented in our phylogeny, considering the total number (13) of described species. The dentate condition of the mandible in the emarginatus species group is considered plesiomorphic for the genus (Brown, 1978), whereas the decrease or loss of these teeth is considered a derived condition. Brown (1978) believed that the arboreal habit of emarginatus group species is a primitive condition shared with Old World *Anochetus* species, which also have long, developed mandibular teeth.

Clade I includes the inermis, bispinosus and mayri species groups and, as in Larabee *et al.* (2016), contains a polyphyletic grouping. In the basalmost divergence, the sister of the remaining species is *A. simoni*, which has been assigned to the inermis species group. In the next, more-recent divergence *A. bispinosus* (bispinosus species group) is the sister of the remaining species with good support (BPP: 0.99), but the remaining species include a group of specimens identified as *Anochetus* cf. *simoni* with maximum support (BPP: 1), rendering the inermis species group polyphyletic (Fig. 2). The specimens of *Anochetus* cf. *simoni* correspond to a new species (unpublished data) and are morphologically close to *A. bispinosus*, with the mesosoma and petiole rugose.

The node uniting the inermis and mayri groups has high support (BPP: 99, rBS: 84, gBS: 82). The species *Anochetus* cf. *targionii* differs morphologically from *A. targionii*, including in the degree of pilosity and mesosomal sculpture, and possibly represents a separate undescribed species.

Clade H was calibrated with the fossils *A. exstinctus* and *A. ambiguus* (Fig. 3), whereas clade I was calibrated with the species *A. dubius* from Dominican amber (estimated date of 17 Ma). The two clades originated and diversified almost simultaneously, 33 and 30–29 Ma for the groups emarginatus

and mayri, respectively, a result similar to that of Larabee *et al.* (2016). Both clades have short branch lengths, suggesting that some groups have experienced rapid radiation in the last 30 Ma, with a common ancestor in the Indomalayan region during the early Eocene.

The topology of the clade J agrees with that of Larabee *et al.* (2016), including the position of *A*. cf. *madaraszi*, which is strongly supported in both studies. *Anochetus* cf. *madaraszi* requires further study because it is a possible new species, morphologically distinct from *A. madaraszi* (sedilloti species group) (Fig. 2). The grandidieri species group was recovered with high support values (gBS: 95, rBS: 100, BPP: 1). Species in this group have an axially compressed petiole and small eyes. Because these character states are less clearly assignable to *A. katonae*, its inclusion in the grandidieri group by Brown (1978) appeared questionable at the time. Due the position of *A. katonae* and *A*. cf. *grandidieri*, the grandidieri species group is nonmonophyletic in our analyses. The rectangularis species group is composed of individuals of medium size, with the petiole not compressed axially, and in some species, the apex of the petiole bidentate or bicuspid (*A. paripungens* and *A. rectangularis*). Some species (*A. alae* and *A. victoriae*), as described by Shattuck & Slipinska (2012), share the presence of large eyes and a bidentate or bicuspid petiole, with exception of *A. turneri* (petiole axially compressed), recovered in our analyses as well as in those of Larabee *et al.* (2016) as closely related to the graeffei species group. According to our results, as well as those of Larabee *et al.* (2016), we suggest the inclusion of *A. turneri* to the graeffei species group.

In the same clade, the ghilianii species group was recovered with good support (gBS: 99, rBS: 100, BPP: 1), but it consists of three specimens of *A. ghilianii* and therefore does not provide an adequate test of the group created by Brown (1978). Species in the ghilianii group are medium to large in size, have large to medium eyes, the striation of the head does not reach the vertex, and the form of the petiole ranges from axially long to thick. Another highly diverse group that was recovered in our analyses is the africanus group, containing many undescribed species. The africanus group is morphologically close to the ghilianii group, differing only in the conical petiole and the striations of the head reaching the vertex. Brown (1978) divided the africanus species group into two subgroups, africanus and pellucidus, but the pellucidus subgroup was not recovered in our analyses. In our analyses, the species *A. boltoni* and *A. goodmani* were found related to ghilianii and grandidieri groups, but due to absence of shared characters, we decided to include them in africanus group, which includes *A. madagascarensis* (same distribution). Probably future study, targeting the species found on the islands will find that species belongs to some subgroup or a new group.

The graeffei species group was initially proposed by Brown (1978) for medium- to modest-sized ants with small eyes and sculptured bodies. Based on our results, we propose a new composition of the graeffei species group, based on the aforementioned characters as well as a sculptured vertex and pronotum, and petiole axially compressed, to include the species *A. pattersoni*, *A. pubescens*, *A. turneri* and *A. yerburyi*. Clade J is highly variable morphologically and relationships of the sampled species were not well supported, for example, the species *A*. cf. *ruginotus* (graeffei species group) was found to be closely related to *A. obscurior* (sedilloti species group) and *A. pupulatus* (longifossatus species group) within the graeffei species group. Based on morphological study, clade J still includes several undescribed species, emphasizing the need for a revision of the group.

Based on our analyses, clade J is one of the oldest clades, with an estimated origin of 44 Ma (Fig. 3). It is incredibly variable morphologically and is spread across the Afrotropics, Australasia and throughout Southeast Asia. Previous studies (Brown, 1978; Schmidt, 2013; Larabee *et al.*, 2016) suggested that a species in clade J might represent an early diverging, 'ancestral' lineage in *Anochetus*, but this is contradicted by our results.

Much of the evolutionary history of *Anochetus* and *Odontomachus* has yet to be clarified. For example, the sister group remains to be identified with a high degree of confidence, taking into account evidence from phylogeny and biogeography (Fig. S3). Many specimens remain to be described, as evidenced by the recent discovery of *A. hohenbergiae*, some of which may provide critical evidence about the evolutionary history of the two genera, and the discovery of new species may be the most promising way forward for better understanding the evolutionary history of *Anochetus* and *Odontomachus*. This is the first study to include a more representative number of *Anochetus* and *Odontomachus* species and species groups, enabling an examination of Brown's (1976, 1978) proposals and employing multiple methods to reconstruct internal relationships, divergence times and biogeography. It is our hope that future studies will be able to use this phylogenetic hypothesis as a framework for answering a variety of evolutionary questions, including the origin and diversification of trap-jaw mandibles.

Supporting Information

Additional supporting information may be found online in the Supporting Information section at the end of the article.

Figure S1. Phylogeny of trap-jaw ants in the genera *Anochetus* (red branches) and *Odontomachus* (green branches) based on maximum-likelihood analysis conducted in RAxML. Nodal support values indicate maximum-likelihood bootstrap values (rBS).

Figure S2. Phylogeny of trap-jaw ants in the genera *Anochetus* (red branches) and *Odontomachus* (green branches) based on maximum-likelihood analysis conducted in GARLI. Nodal support values indicate maximum-likelihood bootstrap values (gBS).

Figure S3. DEC model: Ancestral biogeographic reconstruction of *Anochetus* and *Odontomachus*. Topology is the maximum credibility tree from the FDB analysis. Clades and nodes with estimated origins and divergences are indicated by the labels: F: Afrotropical; I: Indomalayan; A: Autralasian; P: Palearctic; T: Neotropical; N: Nearctic.

Table S1. List of sampled outgroup and ingroup (*Anochetus* and *Odontomachus*) specimens, indicating DNA voucher specimens and GenBank accession numbers for DNA sequences. Specimens marked with '*' are type material.

Table S2. Primers used for sequencing mitochondrial (*cytochrome oxidase I* – **COI**) and nuclear (*Long-wavelength rhodopsin* – **LW Rh**; *Topoisomerase I* – **TOPI**; *Rudimentary* – **CAD** and *Wingless* – **Wg**) gene fragments in ants.

Table S3. List of 24 sampled specimens ultimately excluded from phylogenetic analyses due to excessive missing data that significantly (negatively) affected the analyses.

Table S4. Partitions and models identified by PartitionFinder v1.1.1 (Lanfear *et al.*, 2012) for the 221 specimens used in the Bayesian (upper table) and RAxML (lower table) analyses of the 4258 bp concatenated dataset. The models employed in the MrBayes analyses (upper table, column 4) are the models available in MrBayes that are closest to the models identified by PartitionFinder (upper table, column 3).

Acknowledgements

We are grateful to many collaborators who donated or loaned specimens: B. L. Fisher, A. Jesovnik, J. T. Longino, H. Bharti, A. Z. Riverón, T. Delsinne, Z. Dominique, A.Y. Harada, R. Sivestre, P. S Robson, C. Rabeling, R. E. Vicente and M. Vasconcelos. We thank J. Sosa-Calvo for his comments for improving early drafts of the manuscript. We are also grateful to the three anonymous reviewers who improved the manuscript with their suggestions and questions. We thank the editor Shaun L. Winterton for the valuable suggestions in the manuscript. IOF is very grateful for the assistance provided by M.W. Lloyd in the SI Laboratories of Analytical Biology and E. Okonski in the SI AntLab, and N. Matzke for the assistance with BioGeoBEARS package. IOF was supported by CAPES/PDSE scholarship 99999.005751/2014-04, a PhD scholarship from CAPES and CNPq. IOF was also funded by an Ernst Mayr Travel Grant (2014) from Harvard University, by Universal Amazonas FAPEAM 30/2013 - 062.01951/2015, PROAP (CAPES) - Finance Code 001 and POSGRAD (FAPEAM). FJL was supported by the U.S. National Science Foundation grant DEB 1407279 and by a Peter Buck Foundation Fellowship. MLO and JHCD acknowledge their research grant from CNPq (processes 306100/2016-9 and 304629/2018-9, respectively). TRS was supported by the U.S. National Science Foundation grants DEB 0949689, DEB 1456964 and DEB 1927224. The authors confirm that there are no disputes over the ownership of the data presented in the paper, and all contributions have been attributed appropriately.

Data availability statement

The data that supports the findings of this study are available in the supplementary material of this article. Gene sequences are available on GenBank under accession numbers MT655576-MT655740 (COI), MT679793-MT679947 (TOPI), MT763963-MT764104/MT764105-MT764115 (LW Rh), MT780314-MT780474/MT780475-MT780482/MT780483-MT780490 (Wg), MT872815-MT872953/MT828489-MT828538 (CAD) also listed in Table S1.

References

Aberer, A.J., Krompab, D & Stamakis, A. (2011) RogueNaRok: An Efficient and Exact Algorithm for Rogue Taxon Identification. https://github.com/aberer/RogueNaRok/wiki.

Almeida, E.A.B., Pie, M.R., Brady, S.G. & Danforth, B.N. (2012) Biogeography and diversification of colletid bees (hymenoptera: Colletidae): emerging patterns from the southern end of the world. *Journal of Biogeography*, **39**, 526–544.

Arcila, D., Pyron, A.R., Tyler, J.C., Orti, G. & Betancur-R, R. (2015) An evaluation of fossil tip-dating versus node-age calibrations in tetraodontiform fishes (Teleostei: Percomorphaceae). *Molecular Phylogenetics and Evolution*, **82**, 131–145.

Asher, R.J., McKenna, M.C., Emry, R.J., Tabrum, A.R. & Kron, D.G. (2002) Morphology and relationships of *Apternodu*s and other extinct zalambdodont placental mammals. *Bulletin of the American Museum of Natural History*, **273**, 1–117.

Asher, R.J., Novacek, M.J. & Geisler, J.H. (2003) Relationships of endemic African mammals and their fossil relatives based on morphological and molecular evidence. *Journal of Mamalian Evolution*, **10**(1/2), 131–194.

Baroni Urbani, C. (1980) *Anochetus corayi* n. sp., the first fossil Odontomachiti ant. (Amber collection Stuttgart: hymenoptera, Formicidae. II: Odontomachiti). *Stuttgarter Beiträge zur Naturkunde. Serie B. Geologie und Paläontologie*, **55**, 1–6.

Berger, M.P. & Munson, P.J. (1991) A novel randomized iterative strategy for aligning multiple protein sequences. *Bioinformatics*, **7**, 479–484.

Boudinot, B.E., Probst, R.S., Brandão, C.R.F., Feitosa, R.M. & Ward, P.S. (2016) Out of the neotropics: newly discovered relictual species sheds light on the biogeographical history of spider ants (*LeptoMarmex*, Dolichoderinae, Formicidae). *Systematic Entomology*, **41**, 658–671. https://doi.org/10.1111/syen.12181.

Borowiec, M.L. (2016) Generic revision of the ant subfamily Dorylinae (hymenoptera, Formicidae). *ZooKeys*, **608**, 1–280.

Borowiec, M.L., Rabeling, C., Brady, S.G., Fisher, B.L., Schultz, T.T. & Ward, P.S. (2019) Compositional heterogeneity and outgroup choice influence the internal phylogeny of the ants. *Molecular Phylogenetics and Evolution*, **134**, 111–121. https://doi.org/10.1016/j.ympev.2019.01.024.

Brady, S. (2003) Evolution of the army ant syndrome: the origin and long-term evolutionary stasis of a complex of behavioral and reproductive adaptations. *Proceedings of the National Academy of Sciences of the U. S. A*, **100**, 6575–6579.

Brady, S.G., Schultz, T.R., Fisher, B.L. & Ward, P.S. (2006) Evaluating alternative hypotheses for the early evolution and diversification of ants. *Proceedings of the National Academy of Sciences of the U. S. A*, **103**, 18172–18177.

Brady, S.G., Fisher, B.L., Schultz, T.R. & Ward, P.S. (2014) The rise of army ants and their relatives: diversification of specialized predatory doryline ants. *BMC Evolutionary Biology*, **14**, 93.

Blaimer, B.B. (2012) Acrobat ants go global–origin, evolution, and systematics of the genus Crematogaster (hymenoptera: Formicidae). *Molecular Phylogenetics and Evolution*, **65**, 421–436.

Blaimer, B.B., Brady, S.G., Schultz, T.R., Lloyd, M.W., Fisher, B.L. & Ward, P.S. (2015) Phylogenomic methods outperform traditional multi-locus approaches in resolving deep evolutionary history: a case study of formicine ants. *BMC Evolutionary Biology*, **15**, 271–285. https://doi.org/10.1186/s12862-015-0552-5.

Bolton, B. (2020) An online catalog of the ants of the world. http://antcat.org (accessed 12 October 2020).

Branstetter, M.G. (2012) Origin and diversification of the cryptic ant genus *Stenamma* Westwood (hymenoptera: Formicidae), inferred from multilocus molecular data, biogeography, and natural history. *Systematic Entomology*, **37**, 478–496.

Bouckaert, R., Heled, J., Kühnert, D. *et al.* (2014) BEAST 2: a software platform for bayesian evolutionary analysis. *PLoS Computational Biology*, **10**, e1003537.

Brown, W.L. Jr (1973) A comparison of the Hylean and Congo-west African rain forest ant faunas. *Tropical Forest Ecosystems in Africa and South America: A Comparative Review* (ed. by B.J. Meggers, E.S. Ayensu and W.D. Duckworth), pp. 161–185. Smithsonian Institution Press, Washington, D.C.

Brown, W.L. Jr (1976) Contributions toward a reclassification of the Formicidae. Part VI. Ponerinae, tribe Ponerini, subtribe Odontomachiti. Section a. introduction, subtribal characters. Genus *Odontomachus*. *Studia Entomologica*, **19**, 67–171.

Brown, W.L. Jr (1977) A supplement to the world revision of *Odontomachus* (hymenoptera: Formicidae). *Psyche (Cambridge)*, **84**, 281–285.

Brown, W.L. Jr (1978) Contributions toward a reclassification of the Formicidae. Part VI. Ponerinae, tribe Ponerini, subtribe Odontomachiti. Section B. genus *Anochetus* and bibliography. *Studia Entomologica*, **20**, 549–652.

Camargo, R.X. & Oliveira, P.S. (2012) Natural history of the Neotropical arboreal ant, *Odontomachus hastatus*: nest sites, foraging schedule, and diet. *Journal of Insect Science*, **12**, 1–9.

Cardoso, D.C., Pompolo, S.D.G., Cristiano, M.P. & Tavares, M.G. (2014) The role of fusion in ant chromosome evolution: insights from cytogenetic analysis using a molecular phylogenetic approach in the genus *Mycetophylax*. *PLoS One*, **9**, e87473.

Cerquera, L.M. & Tschinkel, W.R. (2010) The nest architecture of the ant *Odontomachus brunneus*. *Journal of Insect Science*, **10**, 1–12.

Cox, C.B. (2001) The biogeographic regions reconsidered. *Journal of Biogeography*, **28**, 511–523.

De Andrade, M.L. (1994) Fossil Odontomachiti ants from The Dominican Republic (Amber collection Stuttgart: hymenoptera, Formicidae. VII: Odontomachiti). *Stuttgarter Beiträge zur Naturkunde. Serie B. Geologie und Paläontologie*, **199**, 1–28.

De la Mora, A., Pérez-Lachaud, G. & Lachaud, J.P. (2008) Mandible strike: the lethal weapon of *Odontomachus opaciventris* against small prey. *Behavioral Processes*, **78**, 64–75.

Donoghue, M.J. (1989) The importance of fossils in phylogeny reconstruction. *Annual Review of Ecology, Evolution, and Systematics*, **20**, 431–460.

Drummond, A.J., Suchard, M.A., Xie, D. & Rambaut, A. (2012) Bayesian Phylogenetics with BEAUti and the BEAST 1.7. *Molecular Biology and Evolution*, **29**, 1969–1973.

Feitosa, R.M., Lacau, S., Da Rocha, W.D., Oliveira, A.R. & Delabie, J.H.C. (2012) A giant new arboreal species of the ant genus Anochetus from Brazil (Formicidae: Ponerinae). *Annales de la Société entomologique de France*, **48**, 253–259.

Gotoh, O. (1993) Optimal alignment between groups of sequences and its application to multiple sequence alignment. *Computer Applications in the Biosciences*, **9**, 361–370.

Gronenberg, W. (1996) The trap-jaw mechanism in the dacetine ants *Daceton armigerum* and *Strumigenys* sp. *Journal of Experimental Biology*, **199**, 2021–2033.

Gronenberg, W. & Ehmer, B. (1996) The mandible mechanism of the ant genus *Anochetus* (hymenoptera, Formicidae) and the possible evolution of trap-jaws. *Zoology*, **99**, 153–162.

Guénard, B., Weiser, M., Gomez, K., Narula, N. & Economo, E.P. (2017) The global ant biodiversity informatics (GABI) database: a synthesis of ant species geographic distributions. *Myrmecological News*, **24**, 83–89.

Heath, T.A., Huelsenbeck, J.P. & Stadler, T. (2014) The fossilized birth–death process for coherent calibration of divergence-time estimates. *Proceedings of the National Academy of Sciences, USA*, **111**, E2957–E2966.

Hoenle, P.O., Lattke, J.E., Donoso, D.A. *et al.* (2020) *Odontomachus davidsoni* sp. nov. (hymenoptera, Formicidae), a new conspicuous trap-jaw ant from Ecuador. *ZooKeys*, **948**, 75–105. https://doi.org/10.3897/zookeys.948.48701.

Katoh, K., Misawa, K., Kuma, K. & Miyata, T. (2002) MAFFT: a novel method for rapid multiple sequence alignment based on fast Fourier transform. *Nucleic Acids Research*, **30**, 3059–3066.

Katoh, K., Asimenos, G. & Toh, H. (2009) Multiple alignment of DNA sequences with MAFFT. *Methods in Molecular Biology*, **537**, 39–64.

Katoh, K. & Toh, H. (2010) Parallelization of the MAFFT multiple sequence alignment program. *Bioinformatics*, **26**, 1899–1900.

Katoh, K. & Standley, D.M. (2013) MAFFT multiple sequence alignment software version 7: improvements in performance and usability. *Molecular Biology and Evolution*, **30**, 772–780.

Keller, R.A. (2011) A phylogenetic analysis of ant morphology (hymenoptera: Formicidae) with special reference to the poneromorph subfamilies. *Bulletin of the American Museum of Natural History*, **355**, 1–90.

Krosch, M.N., Baker, A.M., Mather, P.B. & Cranston, P.S. (2011) Systematics and biogeography of the Gondwanan Orthocladiinae (Diptera: Chironomidae). *Molecular Phylogenetics and Evolution*, **59**, 458–468.

Kumar, S. & Hedges, S.B. (1998) A molecular timescale for vertebrate evolution. *Nature*, **392**, 917–920.

Lanfear, R., Calcott, B., Ho, S.Y.W. & Guindon, S. (2012) Partition-finder: combined selection of partitioning schemes and substitution models for phylogenetic analyses. *Molecular Biology and Evolution*, **29**, 1695–1701.

Larabee, F.J. & Suarez, A.V. (2014) The evolution and functional morphology of trap-jaw ants (hymenoptera: Formicidae). *Myrmecological News*, **20**, 25–36.

Larabee, F.J., Fisher, B.L., Schmidt, C.A., Matos-Maraví, P., Janda, M. & Suarez, A.V. (2016) Molecular phylogenetics and diversification of trap-jaw ants in the genera *Anochetus* and *Odontomachus* (hymenoptera: Formicidae). *Molecular Phylogenetics and Evolution*, **103**, 143–154.

Lemmon, A.R. & Moriarty, E.C. (2004) The importance of proper model assumption in Bayesian phylogenetics. *Systematic Biology*, **53**, 265–277.

McCulloch, G.A., Wallis, G.P. & Waters, J.M. (2016) A time-calibrated phylogeny of southern hemisphere stoneflies: testing for Gondwanan origins. *Molecular Phylogenetics and Evolution*, **96**, 150–160.

Maddison, W.P. & Maddison, D.R. (2015) Mesquite: a modular system for evolutionary analysis. Version 3.3. http://mesquiteproject.org.

Marshall, D.C., Simon, C. & Buckley, T.R. (2006) Accurate branch length estimation in partitioned Bayesian analyses requires accommodation of among-partition rate variation and attention to branch length priors. *Systematic Biology*, **55**, 993–1003.

Marshall, D.C. (2010) Cryptic failure of partitioned Bayesian phylogenetic analyses: lost in the land of long trees. *Systematic Biology*, **59**, 108–117.

Matos-Maraví, P., Matzke, N.J., Larabee, F.J. *et al.* (2018) Taxon cycle predictions supported by model-based inference in indo-Pacific

trap-jaw ants (hymenoptera: Formicidae: *Odontomachus*). *Molecular Ecology*, **27**, 4090–4107. https://doi.org/10.1111/mec.14835.

Matzke, N.J. (2013) Probabilistic historical biogeography: new models for founder-event speciation, imperfect detection, and fossils allow improved accuracy and model-testing. *Frontiers of Biogeography*, **5**, 242–248.

Matzke, N.J. (2014) Model selection in historical Biogeography reveals that founder-event speciation is a crucial process in Island clades. *Systematic Biology*, **63**, 951–970.

Mayr, G. (1861) Die Europäischen Formiciden. (Ameisen.): 80 pp. Wien. [(31.xii).1861].

Mehdiabadi, N.J., Mueller, U.G., Brady, S.G., Himler, A.G. & Schultz, T.R. (2012) Symbiont fidelity and the origin of species in fungus-growing ants. *Nature Communications*, **3**, 840–840.

Miller, M.A., Pfeiffer, W. & Schwartz, T. (2010) Creating the CIPRES science gateway for inference of large phylogenetic trees. *Proceedings of the Gateway Computing Environments Workshop* (GCE) IEEE, pp. 1–8.

Molet, M., Peeters, C. & Fisher, B.L. (2007) Permanent loss of wings in queens of the ant *Odontomachus coquereli* from Madagascar. *Insectes Sociaux*, **54**, 183–188.

Moreau, C.S., Bell, C.D., Vila, R., Archibald, S.B. & Pierce, N.E. (2006) Phylogeny of the ants: diversification in the age of angiosperms. *Science*, **312**, 101–104.

Moreau, C.S. & Bell, C.D. (2013) Testing the museum versus cradle tropical biological diversity hypothesis: phylogeny, diversification, and ancestral biogeographic range evolution of the ants. *Evolution*, **67**, 2240–2257.

Patek, S.N., Baio, J.E., Fisher, B.L. & Suarez, A.V. (2006) Multifunctionality and mechanical origins: ballistic jaw propulsion in trap-jaw ants. *Proceedings of the National Academy of Sciences, USA*, **103**, 12787–12792.

Penn, O., Privman, E., Ashkenazy, H., Landan, G., Graur, D. & Pupko, T. (2010) GUIDANCE: a web server for assessing alignment confidence scores. *Nucleic Acids Res*, **38**, W23–W28. https://doi.org/10.1093/nar/gkq443.

Pie, M.R. (2016) The macroevolution of climatic niches and its role in ant diversification. *Ecological Entomology*, **41**, 301–307.

Privman, E., Penn, O. & Pupko, T. (2012) Improving the performance of positive selection inference by filtering unreliable alignment regions. *Molecular Biology and Evolution*, **29**, 1–5.

Raimundo, R.L.G., Freitas, A.V.L. & Oliveira, P.S. (2009) Seasonal patterns in activity rhythm and foraging ecology in the neotropical forest-dwelling ant, *Odontomachus chelifer* (Formicidae: Ponerinae). *Annals of the Entomological Society of America*, **102**, 1151–1157.

Rambaut, A. & Drummond, A.J. (2007) Tracer v1.4. http://beast.bio.ed.ac.uk/Tracer (accessed in 2015).

Rambaut, A., Suchard, M.A., Xie, D. & Drummond, A.J. (2014) Tracer v1.6. [WWW document]. http://beast.bio.ed.ac.uk/Tracer (accessed in 2016).

Ree, R.H. & Smith, S.A. (2008) Maximum likelihood inference of geographic range evolution by dispersal, local extinction, and clodogenesis. *Systematic Biology*, **57**, 4–14.

Ronquist, F., Huelsenbeck, J.P. & Teslenko, M. (2013) MrBayes. Version 3.2.2. http://mrbayes.sourceforge.net/download.php.

Ronquist, F., Teslenko, M., van der Mark, P. *et al.* (2012) MrBayes 3.2: efficient Bayesian phylogenetic inference and model choice across a large model space. *Systematic Biology*, **61**, 539–542.

Santos, I.S., Costa, M.A., Mariano, C.S.F., Delabie, J.H.C., Andrade-Souza, V. & Silva, J.G. (2010) A cytogenetic approach to the study of neotropical Odontomachus and Anochetus ants (hymenoptera: Formicidae). *Annals of the Entomological Society of America*, **103**, 424–429.

Schmidt, C. (2009) Molecular Phylogenetics and Taxonomic Revision of Ponerine Ants (Hymenoptera: Formicidae: Ponerinae) PhD Dissertation. University of Arizona, p. 279.

Schmidt, C. (2013) Molecular phylogenetics of ponerine ants (hymenoptera: Formicidae: Ponerinae). *Zootaxa*, **3647**, 201–250.

Schmidt, C.A. & Shattuck, C.O. (2014) The higher classification of the ant subfamily Ponerinae (hymenoptera: Formicidae), with a review of ponerine ecology and behavior. *Zootaxa*, **3817**, 1–242.

Sela, I., Ashkenazy, H., Katoh, K. & Pupko, T. (2015) GUIDANCE2: accurate detection of unreliable alignment regions accounting for the uncertainty of multiple parameters. *Nucleic Acids Research*, **43**, W7–W14. https://doi.org/10.1093/nar/gkq443.

Shattuck, S.O. & Slipinska, E. (2012) Revision of the Australian species of the ant genus *Anochetus* (hymenoptera: Formicidae). *Zootaxa*, **3426**, 1–28.

Sorger, D.M. & Zettel, H. (2011) On the ants (hymenoptera: Formicidae) of the Philippine Islands: V. the genus *Odontomachus* Latreille, 1804. *Myrmecological News*, **14**, 141–163.

Sosa-Calvo, J., Ješovnik, A., Vasconcelos, H.L., Bacci, M. Jr & Schultz, T.R. (2017) Rediscovery of the enigmatic fungus-farming ant "M*yacetosoritis*" *asper* Mayr (hymenoptera: Formicidae): implications for taxonomy, phylogeny, and the evolution of agriculture in ants. *PLoS One*, **12**, e0176498.

Sosa-Calvo, J., Schultz, T.R., Ješovnik, A., Dahan, R.A. & Rabeling, C. (2018a) Evolution, systematics, and natural history of a new genus of cryptobiotic fungus-growing ants. *Systematic Entomology*, **43**, 549–567.

Sosa-Calvo, J., Fernández, F. & Schultz, T.R. (2018b) Phylogeny and evolution of the cryptic fungus-farming ant genus *Myrmicocrypta* F. Smith (hymenoptera: Formicidae) inferred from multilocus data. *Systematic Entomology*, **44**, 139–162. https://doi.org/10.1111/syen.12313.

Spagna, J.C., Vakis, A.I., Schmidt, C.A., Patek, S.N., Zhang, X., Tsutsui, N.D. & Suarez, A.V. (2008) Phylogeny, scaling, and the generation of extreme forces in trap-jaw ants. *The Journal of Experimental Biology*, **211**, 2358–2368.

Stadler, T. (2010) Sampling-through-time in birth–death trees. *Journal of Theoretical Biology*, **267**, 396–404.

Stamatakis, A. (2014) RAxML version 8: a tool for phylogenetic analysis and post-analysis of large phylogenies. *Bioinformatics*, **30**, 1312–1313.

Villet, M.H. & Wildman, M.H. (1991) Division of labour in the obligately queenless ant *Pachycondyla krugeri* (=*Bothroponera krugeri*) Forel 1910 (hymenoptera Formicidae). *Tropical Zoology*, **4**, 233–250.

Wappler, T., Dlussky, G.M., Engel, M.S., Prokop, J. & Knor, S. (2014) A new trap-jaw ant species of the genus *Odontomachus* (hymenoptera: Formicidae: Ponerinae) from the early Miocene (Burdigalian) of The Czech Republic. *Paläontologische Zeitschrift*, **88**, 495–502.

Ward, P.S. & Sumnicht, T.P. (2012) Molecular and morphological evidence for three sympatric species of Leptanilla (hymenoptera: Formicidae) on the Greek Island of Rhodes. *Myrmecological News*, **17**, 5–11.

Ward, P.S., Brady, S.G., Fisher, B.L. & Schultz, T.R. (2010) Phylogeny and biogeography of dolichoderine ants: effects of data partitioning and r relict specimens on historical inference. *Systematic Biology*, **59**, 342–362.

Ward, P.S., Brady, S.G., Fisher, B.L. & Schultz, T.R. (2015) The evolution of Maymicine ants: phylogeny and biogeography of a hyperdiverse ant clade (hymenoptera: Formicidae). *Systematic Entomology*, **40**, 61–81.

Ward, P.S., Blaimer, B.B. & Fisher, B.L. (2016) A revised phylogenetic classification of the ant subfamily Formicinae (hymenoptera: Formicidae), with resurrection of the genera *Colobopsis* and *Dinomyrmex*. *Zoospecimens*, **4072**, 343–357.

Wilson, E.O. (1959) Adaptive shift and dispersal in a tropical ant fauna. *Evolution*, **13**, 122–144. https://doi.org/10.1111/j.1558-5646.1959.tb02996.x.

Wilson, E.O. (1961) The nature of the taxon cycle in the Melanesian ant fauna. *The American Naturalist*, **95**, 169–193. https://doi.org/10.1086/282174.

Winterton, S.L. & Ware, J.L. (2015) Phylogeny, divergence times and biogeography of window flies (Scenopinidae) and the therevoid clade (Diptera: Asiloidea). *Systematic Entomology*, **40**, 491–519.

Zhang, J. (1989) *Fossil Insects from Shanwang, Shandong, China (In Chinese)*. Shandong Science and Technology Publishing House, Jinan, China. 459 p.

Zhang, J.-X. & Maddison, W.P. (2013) Molecular phylogeny, divergence times and biogeography of spiders of the subfamily Euophryinae (Araneae: Salticidae). *Molecular Phylogenetics and Evolution*, **68**, 81–92.

Zettel, H. (2012) New trap-jaw ant species of *Anochetus* Mayr, 1861 (hymenoptera: Formicidae) from the Philippine Islands, a key and notes on other species. *Myrmecological News*, **1**, 157–167.

Zwickl, D.J. (2006) GARLI: Genetic Algorithm Approaches for the Phylogenetic Analysis of Large Biological Sequence Datasets under the Maximum Likelihood Criterion. Ph.D. dissertation, The University of Texas at Austin.

Zwickl, D.J. (2011) GARLI 2.0. https://www.nescent.org/wg_garli/main_page (accessed in 2015).

Zuckerkandl, E. (1987) On the molecular evolutionary clock. *Journal of Molecular Evolution*, **26**, 34–46.

Accepted 5 March 2021